Accuracy of Computer Generated Approximations to Julia Sets

John W. Hoggard

Dissertation submitted to the Faculty of the
Virginia Polytechnic Institute and State University
in partial fulfillment of the requirements for the degree of

Doctor of Philosophy
in
Mathematics

John Rossi, Chair
Peter Haskell
Peter Linnell
Robert Olin
Robert Wheeler

July 31, 2000
Blacksburg, Virginia

Keywords: Julia sets, Computer algorithms, Meromorphic functions, Polynomial
Schwarzian derivative, Tangent

Accuracy of Computer Generated Approximations to Julia Sets

John W. Hoggard

(ABSTRACT)

A Julia set for a complex function f is the set of all points in the complex plane where the iterates of f do not form a normal family. A picture of the Julia set for a function can be generated with a computer by coloring pixels (which we consider to be small squares) based on the behavior of the point at the center of each pixel. We consider the accuracy of computer generated pictures of Julia sets. Such a picture is said to be accurate if each colored pixel actually contains some point in the Julia set. We extend previous work to show that the pictures generated by an algorithm for the family λe^z are accurate, for appropriate choices of parameters in the algorithm. We observe that the Julia set for meromorphic functions with polynomial Schwarzian derivative is the closure of those points which go to infinity under iteration, and use this as a basis for an algorithm to generate pictures for such functions. A pixel in our algorithm will be colored if the center point becomes larger than some specified bound upon iteration. We show that using our algorithm, the pictures of Julia sets generated for the family $\lambda \tan(z)$ for positive real λ are also accurate. We conclude with a cautionary example of a Julia set whose picture will be inaccurate for some apparently reasonable choices of parameters, demonstrating that some care must be exercised in using such algorithms. In general, more information about the nature of the function may be needed.

Acknowledgments

I wish to express my thanks to my advisor, Dr. John Rossi, who provided me with the freedom to explore the topics which interested me and also provided me with tremendous support; he always seemed to be able to point me to the information or contacts that I needed. He also seemed to have unlimited amounts of time to discuss my work, read drafts, and make suggestions.

I would also like to thank Dr. Peter Haskell, Dr. Peter Linnell, Dr. Robert Olin, and Dr. Robert Wheeler for serving on my committee.

Contents

List of Figures

Chapter 1

Introduction and Review of Literature

We say a family of functions $\mathcal{F}$ is normal on a given set if every sequence of functions in $\mathcal{F}$ has a subsequence which converges locally uniformly in that set. It is useful to note that by the Arzelà-Ascoli Theorem, being normal in a subset of the Riemann sphere is equivalent to the family being equicontinuous on that subset.

We will consider iterates of functions f on the Riemann sphere. (In other words, the complex plane together with the point at infinity.) For such a function $f(z)$, we will say that $f^n(z) = f(f^{n-1}(z))$, with $f^1(z) = f(z)$. So $f^n(z)$ is the composition of f with itself n times, i.e., $f^n(z) = f \circ f \circ \ldots \circ f(z)$. We will be interested in the family $\{f^n(z)\}_{n=1}^{\infty}$ of all iterates of f.

If all the iterates of a function f are defined and form a normal family in some neighborhood of a point z, then we say z belongs to the Fatou set for f, which we will denote by $F(f)$. If not, and consequently either the family $\{f^n(z)\}$ is not defined or is not a normal family in any neighborhood of z, then we say z is part of the Julia set for f, which we will denote by $J(f)$.

We see immediately from the definitions of the Fatou and Julia sets that the Fatou set must be open and the Julia set (as its complement) must be closed. We also see that the Fatou set of a function is completely invariant; that is, $z \in F(f)$ if and only if $f(z) \in F(f)$. The Julia set is backward invariant: if $f(z) \in J(f)$, then $z \in J(f)$. If we also have the functions defined at all points on the Riemann sphere, then the Julia set is also forward invariant: if $z \in J(f)$, then $f(z) \in J(f)$.

The following theorem is of great use in determining whether or not the iterates of f form a normal family.

Theorem 1 (Montel's Theorem) *If a family of functions meromorphic on a domain omits at least three values from the Riemann sphere, then the family is normal on that domain.*

A proof can be found in [22]. As a special case, we have that if the family of functions is in fact analytic in the region, then the family is normal if at least two different points of the Riemann sphere are omitted, since this family already misses infinity.

We also note that if we conjugate a function f by a Möbius transformation M, we do not change the dynamics in any significant way. (Although we do note that a general meromorphic function may no longer be meromorphic when conjugated, as an essential singularity at infinity may now be moved to a finite point in the complex plane.) Conjugation respects iteration: $(M^{-1} \circ f \circ M)^n(z) = M^{-1} \circ f^n \circ M(z)$. By appealing to equicontinuity on the Riemann sphere, we can see that conjugation by a Möbius transformation does not change normality, in the sense that f^n is normal in a neighborhood of z if and only if $M \circ f^n \circ M^{-1}$ is normal in a neighborhood of $M(z)$.

We will be interested in algorithms for generating representations of Julia sets using a computer. Such algorithms have enjoyed great popularity, and we consider the accuracy of the representations generated. In this, we will follow up on the work of Durkin [13] for the family λe^z, which we will discuss and expand upon in Chapter 2. Then we will consider the family $\lambda \tan(z)$ in a similar way, showing accuracy in Chapter 3 for an algorithm we will develop. Finally, we will consider an example in Chapter 4 of a function for which our algorithm will produce an inaccurate representation of the Julia set, and we summarize some conclusions in Chapter 5.

We now proceed to discuss some results which are known for rational functions, entire functions, and meromorphic functions, and specifically for meromorphic functions with polynomial Schwarzian derivatives. It is the last class of functions with which we will be primarily concerned, so we will focus on properties that generalize to this class. We will end with a theorem about functions with polynomial Schwarzian derivatives which we will used to generate computer pictures of their Julia sets. For general discussions of the properties of the Fatou and Julia sets for rational functions, see either [7] or [23]; for a discussion of entire and meromorphic functions, see [8].

1.1 Rational Functions

For a rational function f, the family of functions $\{f^n(z)\}$ is defined at all points on the sphere. Therefore, the Julia set consists only of those points z where the family is not normal in any neighborhood of z. We will assume throughout that the rational functions we work with will be of degree two or greater.

The Fatou sets for rational functions are strongly related to the types of fixed and periodic points the function has. We call z_0 a fixed point for a function f if $f(z_0) = z_0$. We call a sequence of points $z_0, z_1, \ldots, z_n = z_0$ a cycle of order n if $f(z_i) = z_{i+1}$ and n is the smallest integer such that $f^n(z_0) = z_0$. The z_i are referred to as periodic points, and we note that z_i is a fixed point for the function f^n. We can classify a fixed point z_0 for the function f

follows:

- If $0 < |f'(z_0)| < 1$, we call z_0 an attracting fixed point.
- If $f'(z_0) = 0$, we call z_0 superattracting.
- If $|f'(z_0)| > 1$, we call z_0 a repelling fixed point.
- If $|f'(z_0)| = 1$, we call z_0 an indifferent fixed point. If z_0 is indifferent, we write $f'(z_0) = e^{2\pi i\theta}$ and further characterize such a fixed point as rationally indifferent if θ is rational and as irrationally indifferent if θ is irrational.

The quantity $f'(z_0)$ is sometimes referred to as the multiplier or the eigenvalue for the fixed point z_0.

We can characterize a cycle of order n similarly, based on the value of the derivative of f^n at some point in the cycle. First we note that

$$\begin{aligned}(f^n)'(z_0) &= f'(f^{n-1}(z_0))f'(f^{n-2}(z_0))\cdots f'(z_0)\\ &= f'(z_{n-1})f'(z_{n-2})\cdots f'(z_0)\end{aligned}$$

Thus, we get the same value for the derivative of f^n at any point in the cycle, and we can characterize a cycle (and the periodic points in the cycle) as repelling, attracting, superattracting, rationally indifferent, or irrationally indifferent according to the nature of the fixed point z_0 for the map f^n.

All attracting and superattracting fixed points and cycles are a part of the Fatou set. This follows because in a small neighborhood around an attracting (superattracting) fixed point, the map $f(z)$ is a contraction. Therefore the family of functions $f^n(z)$ map this neighborhood into itself, and all points external to this neighborhood are missed by the family. Similarly the function f^m is a contraction around each point in a cycle of order m. This and the fact that normality for the family $(f^m)^n$ implies normality for the family f^n shows that all attracting and superattracting cycles are in the Fatou set. It is worth noting that superattracting fixed points are different from attracting fixed points in that they are also critical values.

Conversely, all repelling fixed points are in the Julia set. Indeed, conjugating by a suitable Möbius transformation, we may assume that the fixed point is at the origin. Then if we have $|f'(0)| > 1$, we see that if a sequence of iterates converged uniformly in a neighborhood to some function ϕ, it would be necessary for $\phi(0) = 0$, so ϕ would be analytic in a neighborhood of 0, and thus $\phi'(0)$ must be finite. However, we also see that $(f^n)'(0) = (f'(0))^n$ goes to infinity as n does, so it is impossible for the iterates to be normal in a neighborhood of a repelling fixed point. Further, the repelling periodic points are dense in the Julia set. (See for example [7, §6.9].)

Components of the Fatou set may also be invariant (or periodic) in the sense that for some component U we have $f(U) = U$ (or $f^n(U) = U$). We may identify five different types of

such components which appear in the Fatou sets of rational functions. For each type listed below, we also describe the behavior of f on the region:

- *An attracting domain.* An attracting domain contains an attracting fixed point (cycle). On iteration, f (or f^n) tends toward this fixed point (cycle). Attracting domains are sometimes called Schröder domains.
- *A superattracting domain.* Superattracting domains are the same as attracting domains, except they contain a superattracting fixed point (cycle). Superattracting domains are sometimes called Böttcher domains.
- *A Parabolic Domain.* A parabolic domain has a rationally indifferent fixed point on the boundary of the domain, and points in the domain move toward the fixed point under iteration. Parabolic domains are also known as Leau domains.
- *A Siegel Disk.* A Siegel disk is a Fatou component for which the action of f on U is conformally conjugate to a rotation of a disk about the origin. It is necessary for the rotation to be by an irrational root of unity, as otherwise we would have for some n that $f^n(z) = z$ for all $z \in U$, which would imply that the rational function f is degree one.
- *A Herman Ring.* A Herman ring is conformally conjugate to the rotation of an annulus centered at the origin. Again, it is necessary for the rotation to be irrational.

Determining that these are the only possibilities for a cyclic component requires determining what sort of functions the family $\{f^n\}$ may converge to in U. If all convergent subsequences of the family approach only constant functions, then we must have a fixed point, and we get one of the first three situations. If some subfamily approaches other, non-constant functions, it has been shown that either a Siegel Disk or a Herman ring results. (For details, see [7, §7.4].)

An important theorem proved by Sullivan in 1985 [24] states that all Fatou components for a rational function are eventually periodic. That is, for any component U of the Fatou set $F(f)$, there exists some m such that $f^m(U)$ is a periodic component. A component U such that $f^n(U) \not\subseteq f^m(U)$ for any integers $m \neq n$, is called a wandering domain. Thus, Sullivan's result says that rational functions do not have wandering domains.

For polynomials, ∞ is a superattracting fixed point. The multiplier at infinity is defined as the multiplier for $1/f(1/z)$ at the origin, and we see that for a polynomial of degree at least two, this quantity is zero. So in fact, there is a superattracting component of the Fatou set containing infinity for polynomials. Using this fact, the *filled in Julia set* is sometimes defined to be the complement of $I(f) = \{z : f^n(z) \to \infty\}$ in the complex plane. Most computer algorithms for generating pictures of Julia sets for polynomials rely on testing points to

see whether or not $f^n(z)$ becomes large, and coloring those points which stay within some specified bound.

It may be harder to generate computer pictures of the Julia set of a general rational function f. One approach involves iterating the inverse of the function and following the preimage of selected points. It is a consequence of Montel's theorem that if p is any point in the Julia set of a function f, and U is any neighborhood of p, then the union $\cup f^n(U)$ misses at most two points. In fact, the two points are independent of p, and we define these points to be the exceptional points of f. We denote the (possibly empty) set of exceptional points $E(f)$. For rational functions, it is possible to show that $E(f)$ is contained in the Fatou set, although this need not be true for general meromorphic functions. (For example, if z is a pole which is also an omitted value, then $z \in E(f)$, but we will see that z is also in the Julia set.) It can now be seen that if we take any point $z \notin E(f)$, then the preimages $\cup f^{-n}(z)$ of z must accumulate around $J(f)$, since they must appear in any neighborhood of any point of $J(f)$. (This set of all preimages of z $\cup f^{-n}(z)$ is called the backwards orbit of z, and denoted $O^-(z)$.) Consequently, we can say that $J(f) \subset \overline{O^-(z)}$, so long as $z \notin E(f)$. As a consequence of invariance, we have the yet better result that if we choose $z \in J$, then $J(f) = \overline{O^-(z)}$. (See [9, §4] for further details. We note that if f is a more general function for which E may include points in $J(f)$, the proof is still valid as long as we pick $z \in J \backslash E$.)

Therefore, we can take any point (except for the two exceptional points) and find a set of preimages for the point under the functions f^n. These preimages will converge under iteration to the Julia set. If we can determine a point in the Julia set to begin with (such as a repelling fixed point, for example), we can compute the preimages of this point and know that we are in the Julia set. We would expect such algorithms for numerically approximating the Julia set to be relatively stable, since any point other than an exceptional point will have preimages which converge to the Julia set, so any errors in our initial approximation or any subsequent roundoff errors should tend to be wiped out in each iteration.

Computationally, the back iteration technique has three drawbacks. First, we must compute an inverse, which may be difficult or costly. Second, the number of preimages found at each backwards iteration grows exponentially, and it is possible to find multiple preimages within a single pixel, which wastes resources. Thirdly, we have the problem that while the preimages of a non-exceptional point come arbitrarily close to each point in the Julia set, they need not visit each point equally often. Thus, some regions can be filled in more completely than others. A paper by Saupé [21] and a chapter by Peitgen [20] discuss some of these problems and ways to implement computer algorithms which help overcome them.

1.2 Entire Functions

We now turn briefly to functions which are analytic in the complex plane. These functions have some similarity with rational functions, and some notable differences.

First we note that infinity is an essential singularity for transcendental entire functions. (Infinity is in fact in the Julia set for such a function, as it has no forward orbit. However, infinity is also an omitted value for entire functions, so we may think of them as maps from the complex plane to itself.) The singularity at infinity suggests the possibility that points which tend to infinity may be in the Julia set. Eremenko proved [14] that in fact for transcendental entire functions, the set $I(f)$ of points z such that $f^n(z) \to \infty$ is nonempty, and that the boundary of $I(f)$ is equal to the Julia set. There may however be points in $I(f)$ which are in the Fatou set; an example of such points is given by functions with Baker domains, as we will describe.

In addition to the five types of invariant regions described for rational functions, we also have so-called *Baker domains.* A Baker domain is a component of the Fatou set with infinity as a boundary point, and for which $f^n(z) \to \infty$ uniformly on the domain. (See for example [8].) Essentially, a Baker domain is like a parabolic domain, except that the point on the boundary to which the Fatou component converges is not periodic, and indeed has no forward orbit. It is also possible to have an invariant or periodic domain with infinity on the boundary which is (super) attractive, parabolic, or a Siegel disk. Baker and Domínguez [3] discuss such components.

Attracting and superattracting fixed points (cycles) continue to be in the Fatou set for the same reasons as before, and repelling fixed points (cycles) are still in the Julia set. In fact, the repelling periodic points are still dense in the Julia set for entire functions, as Baker proved [1].

Critical points continue to be of significance, but we now find that each Fatou component is associated with either a critical point or an asymptotic value. Call the closure of all asymptotic and critical values for a function f the singular values for f. Then all attractive and parabolic periodic domains for f contain a singular value, and the boundary of any cycle of Siegel disks or Herman rings attracts the infinite forward orbit of a singular value. (See [8]. The proof is an extension of Fatou's proof [16] for rational functions.)

Unfortunately, for entire functions it may be possible to have wandering domains, so not all domains of the Fatou set are pre-periodic. The existence of wandering domains was first shown by Baker [2] in 1976. Other examples can be found in [15].

1.3 Meromorphic Functions

When we have a transcendental meromorphic function with at least one pole, we no longer have a dynamical system. Any preimage of a pole has a finite forward orbit, because infinity is an essential singularity and there is no way to define $f(\infty)$. As a result, all preimages of poles are in the Julia set for such functions.

General meromorphic functions can still have the same types of invariant Fatou components

as entire functions, including Baker domains. (See [6] for details.) Of course, entire functions are meromorphic, but have no poles.

Asymptotic values and critical values still determine the Fatou components. In general, there are still wandering domains. (See [4] for examples of a variety of different types of wandering domains a general meromorphic function may have.)

We consider next the more restricted class of transcendental meromorphic functions with at least one distinct pole that is not an omitted value. (Functions with only one distinct pole which is omitted are of the form $\alpha + (z-\alpha)^{-k}\exp(g(z))$ where g is a non-constant entire function. Such functions are special in that they are analytic self-maps of the punctured plane.) Again denote the set of exceptional values by $E(f)$. We have [5] that $E(f)$ contains only two points, and for any q in the Julia set and any p not in $E(f)$, q is an accumulation point of $O^-(p)$. Thus, the inverse iterates of f converge to the Julia set for any point except for at most two exceptional points, as in the rational case. The set $O^-(\infty)$ is infinite for such functions, and this set is dense in the Julia set [5]. Thus, we may characterize the Julia sets of such functions as the closure of the set of preimages of poles of all orders.

Domínguez proved [12] that for transcendental meromorphic functions, the set of points $I(f)$ which go to infinity under iteration is nonempty and the boundary of this set is the Julia set for the function, as Eremenko showed for entire transcendental functions. (In general, there may also be points in the Fatou set which go to infinity; this is possible either through Baker domains or wandering domains.)

1.4 Functions with Polynomial Schwarzian Derivatives

We finally consider the subset of meromorphic functions which have polynomial Schwarzian derivative. The Schwarzian derivative $S(f)$ for a function is defined as follows:

$$S(f)(z) = -2\frac{(f'(z)^{-1/2})''}{f'(z)^{-1/2}} = \frac{f'''(z)}{f'(z)} - \frac{3}{2}\left(\frac{f''(z)}{f'(z)}\right)^2$$

Since functions with one distinct pole which is also an omitted value cannot have polynomial Schwarzian derivative [11], we note that all the results about meromorphic functions mentioned before still hold. In particular, the repelling periodic points are still dense in the Julia set, the same possibilities for invariant or cyclic components occur as before, and the Julia set is the closure of $O^-(\infty)$.

For our purposes, the significant fact about a function having a polynomial Schwarzian derivative comes from the second theorem of Nevanlinna (see [18] for example), which implies that such a function will have finitely many asymptotic values. In fact, a function whose Schwarzian derivative is a polynomial of order p has exactly $p-2$ asymptotic values, and

such functions have no critical values [11]. These properties limit significantly the behavior of the Fatou components.

First, we note that a proof by Devaney and Keen [11] indicates that meromorphic functions with polynomial Schwarzian derivatives have no wandering domains; i.e., every Fatou component is pre-periodic. In addition, Devaney and Keen also show that such functions do not have Baker domains. (They show in fact that any forward invariant set sufficiently close to infinity is in fact in the Julia set.) It was brought to the author's attention by Aimo Hinkkanen that these are the only ways for a point in the Fatou set to approach infinity, so these results allow us to conclude that any point in $I(f)$ must lie in the Julia set. Combining this fact with Domínguez' result [12] that the boundary of $I(f)$ is equal to the Julia set, we have shown the following for functions with polynomial Schwarzian derivative:

Theorem 2 *For transcendental meromorphic functions with polynomial Schwarzian derivative, the Julia set is equal to the closure of* $I(f) = \{z : f^n(z) \to \infty\}$.

This will provide us with an algorithm for generating computer pictures of Julia sets for such functions, which we will show is sometimes reliable and sometimes not.

Chapter 2

The Family λe^z

We consider the family $E_\lambda(z) = \lambda e^z$. Durkin [13] discussed the accuracy of computer representations of these Julia sets for specific values of λ in the following manner: Select a window W in the complex plane, a real bound B, a bound on iterations N, and a pixel width d. We then compute an approximation to the Julia set of E_λ by dividing W into squares of width d (which we will refer to as pixels), and selecting a point z_0 in the center of a given pixel. We then iterate the function E_λ at the point z_0. If for some $n \leq N$, the n^{th} iterate has a real part greater than B, then we color the pixel. Otherwise, we leave the pixel uncolored. This algorithm is based on the fact (proven by Devaney and Durkin [10]) that for the family λe^z, the Julia set consists of the closure of all points z such that $\operatorname{Re} E_\lambda^n(z) \to \infty$.

We call this approximation the computed Julia set and denote it $J_c(E_\lambda)$. We say that $J_c(E_\lambda)$ is *accurate* if for every pixel which is colored, there is some z^* inside the pixel such that z^* is actually in the Julia set. We note that in general z^* need not be the same as the point z_0 we iterated; it need only be in the same pixel. In other words, each pixel which is colored under the algorithm in fact contains some point in the Julia set.

Durkin established the accuracy of the computed Julia set for the function $0.3\,e^z$ with $B = 50$, $N = 25$, and $W = \{z : 1 \leq \operatorname{Re} z \leq 5, |\operatorname{Im} z| \leq 2\}$, and the accuracy of e^z with the same B, N, and W. (We note however that the case where $\lambda = 1$ is of less immediate interest, as for any $\lambda > 1/e$ the Julia set for $\lambda\, e^z$ is the entire complex plane; see [10].) We will extend her methods to show that, using the same B, N, and W, the Julia sets for $\lambda\, e^z$ are accurate for all values of λ less than $1/e$; i.e., we establish accuracy for all values of λ for which the Julia set $J(E_\lambda)$ is not the whole complex plane.

The choice of W for $\lambda < 1/e$ is worth considering. Restrictions on the imaginary part need not cause concern, as the function is $2\pi i$-periodic. In fact, we could proceed with the same proof if we only restricted ourselves to $|\operatorname{Im} z| < \pi$, which would show us the entire picture. However, we will see when we discuss the structure of the Julia set that it is in fact restricted to the strip $|\operatorname{Im} z| < \pi/2$ and the $2\pi i$-translates, so the given W will show us a complete

picture. The restrictions on the real part of the window are similarly designed to show us the "interesting" part of the Julia set. We note that $\operatorname{Re} E_\lambda(z) = \lambda e^{\operatorname{Re} z} \cos(\operatorname{Im} z)$, and so for $\lambda < 1/e$ and $\operatorname{Re} z < 1$, we have immediately that $\operatorname{Re} E_\lambda(z) < \frac{1}{e} e^1 = 1$. Thus, the region with $\operatorname{Re} z < 1$ always maps to itself, and is consequently in the Fatou set. We additionally see that any pixel which has a center z_0 with $\operatorname{Re} z_0 < 1$ will never be colored by our algorithm. The choice of 5 as the upper bound on the real part is arbitrary.

The general method of our proof that the computed Julia set $J_c(E_\lambda)$ is accurate is based on Durkin's proof for $\lambda = 0.3$ and proceeds as follows. We first determine a set of curves S which we show to be in the Julia set. We then demonstrate that the ball $B_r(z)$ of radius r about z will have non-empty intersection with the set S, provided $\operatorname{Re} z$ and r are sufficiently large. Finally, we demonstrate that if a point z_0 in the center of a pixel is mapped under iteration by E_λ to a point z_n with real part larger than B, then a neighborhood of z_0 within the pixel is expanded enough under iteration by E_λ to contain a ball $B_r(z_n)$ which has large enough $\operatorname{Re} z_n$ and r to intersect $S \subset J(E_\lambda)$. Since the Julia set is backward invariant, the original pixel contained a point in $J(E_\lambda)$.

2.1 The Structure of the Julia set for $E_\lambda(z)$

We begin by determining a sequence of curves which lie in $J(E_\lambda)$. We consider the function λe^x on the real axis, and see that it has, for $0 < \lambda < 1/e$, two fixed points. The left most fixed point, which we will call q_λ, will be attracting (as the derivative is clearly smaller than one) and the right most, which we will denote p_λ, will be repelling. (See figure 2.1.) We note

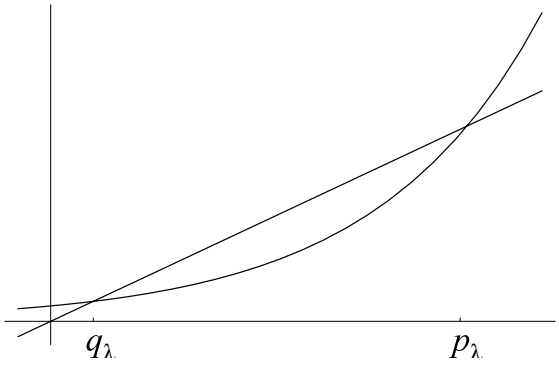

Figure 2.1: Fixed points for e^x: q_λ must be attracting and p_λ must be repelling.

that $[p_\lambda, \infty)$ will be in the Julia set for E_λ. Indeed, p_λ is a repelling fixed point and therefore in $J(E_\lambda)$, and for any real x greater than the fixed point p_λ we can see that $E_\lambda^n(x) \to \infty$ as $n \to \infty$, so x is in $J(E_\lambda)$. Of course since E_λ is $2\pi i$-periodic, we also have $[p_\lambda, \infty) \pm 2n\pi i$ in $J(E_\lambda)$. Conversely, if z has real part less than p_λ, z is in the Fatou set. This follows from the fact that if $x < p_\lambda$, then $\operatorname{Re} \lambda e^{x+iy} = \lambda e^x \cos(y) < \lambda p_\lambda < p_\lambda$, since $\lambda < 1/e < 1$. Thus,

the region $\{z : \operatorname{Re} z < p_\lambda\}$ maps to itself, and by Montel, the family $\{E_\lambda^n\}$ is normal in this region. With these facts in mind, we let γ be a preimage of $\operatorname{Re} z = p_\lambda$, and let c_n be the preimages of $[p_\lambda, \infty) \pm 2n\pi i$. (Without loss of generality, we will usually assume that the preimages c_n are those in the strip of width 2π centered on the real axis.) Then the c_n are curves in $J(E_\lambda)$, and $J(E_\lambda)$ is restricted to the region in the right half-plane bounded by γ and its πi translates. (See figure 2.2.)

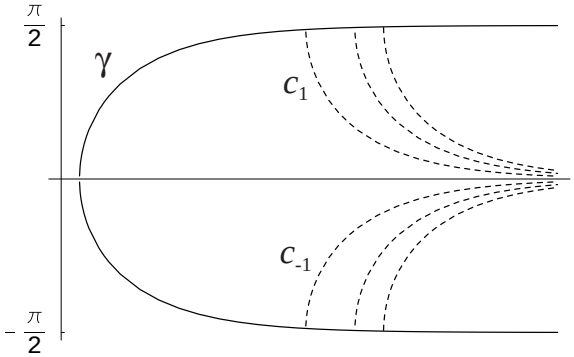

Figure 2.2: The curve γ (preimage of $\operatorname{Re} z = p_\lambda$) and a few of the c_n (preimages of $[p_\lambda, \infty) + 2n\pi$)

2.2 Preliminary Results

We will need the following theorem, proved by Devaney and Durkin [10]:

Theorem 3 (Expansion Theorem) *Suppose $|E'_\lambda(z)| > \mu$ for all $z \in B_\delta(z_0)$ where $\delta < \pi$. Then there is an open set $U \subseteq B_\delta(z_0)$ such that $E_\lambda : U \to B_{\mu\delta}[E_\lambda(z_0)]$ is a homeomorphism.*

In considering the proof of the expansion theorem, we find that the restriction on δ is needed only to be sure that E_λ is one-to-one. A modified version of the expansion theorem will hold for any function that is one-to-one within the ball $B_\delta(z_0)$.

We will also use the following lemma, which is a modification of Lemma 2.2 in Durkin's paper. (Durkin uses a ball of radius two, and λ of 0.3.) We follow the structure of her proof except where we need additional estimates to deal with our more general λ.

Lemma 1 *Let S be the set consisting of the curves c_n (n an integer), the line segment $[p_\lambda, \infty)$, and all $2\pi i$-translates. If $\operatorname{Re} z > 120$ and $e^{-4} \leq \lambda \leq e^{-1}$, then*

$$B_{1.6}(z) \cap S \neq \emptyset$$

where $B_{1.6}(z)$ denotes the ball of radius 1.6 about z.

Proof: We will begin by finding the location of the points of intersection of γ and the c_n. Without loss of generality, we will work in the strip with imaginary part between $-\pi$ and π. To find a representation for γ, we solve for the preimage of $\operatorname{Re} z = p_\lambda$, and we see that γ is given by

$$y = \pm \arccos \frac{p_\lambda}{\lambda e^x}$$

(We therefore additionally see that we have γ with imaginary part between $-\pi/2$ and $\pi/2$, as shown in figure 2.2.)

The equation of each c_n is

$$y = \arcsin \frac{2n\pi}{\lambda e^x}$$

Solving these equations simultaneously leads to a set of points x_n which are the points at which γ and c_n intersect. We will need the location of these points. The x_n are given by

$$x_n = \frac{1}{2} \ln(p_\lambda^2 + 4n^2\pi^2) - \ln \lambda$$

Additionally, we will need to know how close together these points are. We call Δx_n the distance between x_n and x_{n+1}, and by subtracting and simplifying we find that

$$\Delta x_n = x_{n+1} - x_n = \frac{1}{2} \ln \left(\frac{p_\lambda^2 + 4(n+1)^2\pi^2}{p_\lambda^2 + 4n^2\pi^2} \right)$$

We will require estimates of the p_λ to estimate both x_n and Δx_n. We note that $x = p_\lambda$ is where $\lambda e^x - x = 0$. Expanding the Taylor series for λe^x, we find that $\lambda e^x - x > \lambda + (\lambda - 1)x + \frac{\lambda}{2}x^2$. Solving this quadratic for the rightmost solution yields a point

$$\frac{1 - \lambda + \sqrt{1 - \lambda(2 - \lambda)}}{\lambda}$$

which is greater than p_λ. (See figure 2.3.) Since we are assuming $\lambda < 1/e$, we can see that

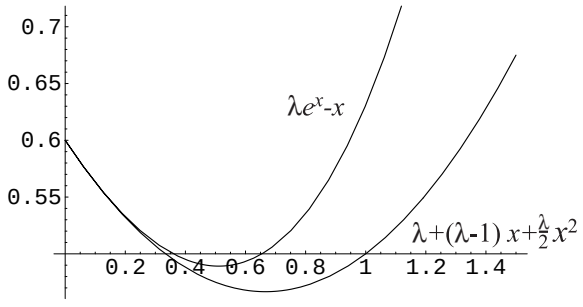

Figure 2.3: An upper bound on p_λ, using the root of a Taylor polynomial

$\lambda(2-\lambda) < (1/e)(2-1/e)$, which in turn is less than $(1/2.7)(2-1/2.8) < .61$, and so our solution to the quadratic is ultimately less than $(1.7/\lambda) - 1$. So we have

$$p_\lambda < \frac{1.7}{\lambda} - 1$$

For $\lambda \geq e^{-4}$ (as we are assuming), p_λ is therefore less than $1.7e^4 - 1 < 1.7(2.8)^4 < 104$. In the other direction, we note that $\lambda e^x \geq \lambda$ for $x \geq 0$, so $p_\lambda \geq \lambda \geq e^{-4} > 1/2.8^4 > .016$. Therefore we have that $.016 \leq p_\lambda \leq 104$.

The points x_n at the intersection of c_n and γ will be the points which we show to be in the ball given in Lemma 1. Since we will be looking at a ball of radius 1.6 and centered at a point with real part greater than 120, we will be working with n large enough that x_n is at least 118. We want to determine how close together the x_n need be if the x_n are this large. Using our estimates for p_λ we get

$$\Delta x_n < \frac{1}{2}\ln\left(\frac{104^2 + 4(n+1)^2(3.2)^2}{(.016)^2 + 4n^2(3.1)^2}\right) = \frac{1}{2}\ln\left(\frac{40.96n^2 + 81.92n + 10,856.96}{38.44n^2 + .000256}\right)$$

We note Δx_n is a decreasing function of n and the x_n are increasing. Since we can easily determine that $x_n < 118$ if $n > 2^{12}$ (for $\lambda \in [e^{-4}, e^{-1}]$), we know that the n we will work with must be larger than this. Therefore, we know that by the time we have reached a ball of radius 1.6 about a point z with real part greater than 120, the spacing between the x_n must be less than $\Delta x_{(2^{12})}$, which means that

$$\Delta x_n < \frac{1}{2}\ln(1.067) < .033$$

(We note that $\frac{1}{2}\ln(1.067) < .033$ because $\ln(1.067) < .066$, where the latter can be confirmed by expanding a Taylor series for e^x about the origin: $e^{.066} > 1 + .066 + (.066)^2/2 = 1.06818$.)

Therefore we can conclude that if we have a ball $B_{1.6}(z)$ of radius 1.6 centered at z with $\operatorname{Re} z \geq 120$, and that ball intersects the curve γ over a set of x values longer than .033, we are guaranteed that the region will intersect the end point of one of the c_n.

Now we consider $B_{1.6}(z)$ with $\operatorname{Re} z > 120$, and we will show that this ball must intersect γ over such a range of x values. (In other words, the projection onto the real axis of the portion of the curve inside the ball is longer than .033.) We see for any R that if $|\operatorname{Im} z| < R$, then $B_R(z)$ will cross $[p_\lambda, \infty)$, which is in S. We will therefore assume $R \leq |\operatorname{Im} z| \leq \pi$. We will continue to work (without loss of generality) with a circle centered at a point z in the strip of width 2π about the real axis. We see that our worst case scenario is where the point z is as far as possible from both γ and its next $2\pi i$-translate. Therefore, we will assume that $|\operatorname{Im} z| = \pi$. Working with our specified $R = 1.6$, we have that the boundary of $B_{1.6}(z)$ intersects γ where

$$(x - \operatorname{Re} z)^2 + \left(\arccos\left(\frac{p_\lambda}{\lambda e^x}\right) - \operatorname{Im} z\right)^2 = 1.6^2$$

which after using the assumption that $\operatorname{Im} z = \pi$ and simplifying somewhat becomes

$$(x - \operatorname{Re} z)^2 + \left(\frac{\pi}{2} + \arcsin\left(\frac{p_\lambda}{\lambda e^x}\right)\right)^2 = 1.6^2$$

We note that there will be at most two intersection points; all the points between the intersections of γ and the boundary of $B_{1.6}(z)$ are inside of $B_{1.6}(z)$.

Next, we need to find an upper bound for $\arcsin\left(p_\lambda/(\lambda e^x)\right)$. We already know that $p_\lambda < (1.7/\lambda) - 1$. Noting that $\arcsin(\theta) < 2\theta$ for $0 < \theta < 1/2$, and that our x is assumed to be greater than 120, we have that

$$\arcsin\left(\frac{p_\lambda}{\lambda e^x}\right) < 2\frac{1.7 - \lambda}{\lambda^2 e^{120}}$$

Given our restriction that $e^{-4} \leq \lambda < e^{-1}$, we can further say that

$$\arcsin\left(\frac{p_\lambda}{\lambda e^x}\right) < 2\frac{1.7 - \lambda}{\lambda^2 e^{120}} < \frac{1.7 - 0}{e^{-8} e^{119}} < \frac{1.7}{e^{111}} < e^{-111}$$

and expanding e^{111} in a Taylor expansion we can determine that this is easily less than .001.

We now return to where our disk intersects γ, and we determine that if we have

$$(x - \operatorname{Re} z)^2 + \left(\frac{\pi}{2} + \arcsin\frac{p_\lambda}{\lambda e^x}\right)^2 > 1.6^2$$

i.e., if a point lies outside the disk of radius 1.6, then we must have

$$(x - \operatorname{Re} z)^2 > 1.6^2 - \left(\frac{\pi}{2} + .001\right)^2 > .089 > (.033)^2$$

So we see that the disk must intersect γ in a segment at least .033 long in the x direction, which is long enough (assuming $x > 120$) to guarantee the existence of some x_n inside the curve. Thus, the disk $B_{1.6}(z)$ must intersect S if $\operatorname{Re} z > 120$, just as we wanted, and the lemma is proved. ■

2.3 Accuracy of $E_\lambda(z)$ for $\lambda < 1/e$

We are now ready to show:

Theorem 4 *The Julia sets computed for $E_\lambda(z)$, $\lambda < 1/e$, using $B = 120$, $N = 25$, $d = .01$, and $W = \{z : 1 \leq \operatorname{Re} z \leq 5, |\operatorname{Im} z| \leq 2\}$ are accurate.*

Proof: We begin with the observation that if $\lambda < e^{-4}$, the picture generated is trivially accurate. This follows because $\operatorname{Re} E_\lambda(z) = \lambda e^{\operatorname{Re} z}\cos(\operatorname{Im} z) < e^{\operatorname{Re} z - 4}$, and within W, we have $\operatorname{Re} z \leq 5$. So we note that the region $\operatorname{Re} z \leq 5$ is mapped to a region with $\operatorname{Re} z \leq e < 5$, and thus it will be impossible for any point in W to be iterated outside of this region (where $\operatorname{Re} z > 120$), so no pixel will be colored under our algorithm. Therefore, in a vacuous sense, the picture is accurate. (Note that the above also implies that the W we have chosen lies entirely in the Fatou set. If we wanted pictures which contained part of the Julia set for these small values of λ, we would need to change our choice of W.)

We now deal with the case of $\lambda \in [e^{-4}, e^{-1})$. In this case, it will be sufficient by Lemma 1 to show that if a pixel is colored, i.e., if there is some $n \leq N$ such that $\operatorname{Re} E_\lambda^n(z) > B = 120$, then the pixel is expanded to cover a ball of radius 1.6 about z. Therefore by Lemma 1 the pixel would have contained some point in the Julia set of E_λ.

We work in cases, considering how many of our $N = 25$ iterations were necessary before $\operatorname{Re} E_\lambda^n(z) > 120$.

Case 1: $n = 1$ Suppose we have $z_0 \in W$ and $\operatorname{Re} E_\lambda(z_0) > 120$. (In other words, we took only one iteration to escape.) We have then that $\lambda e^{x_0}\cos(y_0) > 120$, where $z_0 = x_0 + iy_0$. But then $e^{x_0} > 120/\lambda$, and $x_0 > \ln 120 - \ln\lambda$. Since $\lambda < e^{-1}$, we must have $x > \ln 120 + 1$. But since $\ln 120 > 4.7$, this would mean that the real part of z_0 was bigger than 5.7, which is not possible for $x \in W$. Therefore, no pixel is colored in the first iteration.

Case 2: $n = 2$ Suppose we have a point $z_0 \in W$, with $z_1 = E_\lambda(z_0)$, and $z_2 = E_\lambda^2(z_0)$, such that $\operatorname{Re} z_2 > 120$. Working as in Case 1, we can establish that $\operatorname{Re} z_1 > 4.7 - \ln\lambda$, which means in turn that $\operatorname{Re} z_0 > \ln(4.7 - \ln\lambda) - \ln\lambda$.

We then consider the neighborhood $B_{.005}(z_0)$ under the map E_λ. We note that $E_\lambda'(z) = E_\lambda(z)$, and that for $z \in B_{.005}(z_0)$, $\operatorname{Re} z > \ln(4.7 - \ln\lambda) - .005$. We therefore have that $|E_\lambda'(z)| > (4.7 - \ln\lambda)e^{-.005}$. Letting $\mu_0 = (4.7 - \ln\lambda)e^{-.005}$, we have by the expansion theorem that there is a neighborhood U_1 of z_1 which contains $B_{.005\mu_0}(z_1)$ such that $E_\lambda(z) : B_{.005}(z_0) \to U_1$ is a homeomorphism.

Now we have a disk of radius $.005\mu_0$ around z_1, and since $\operatorname{Re} z_1 > 4.7 - \ln\lambda$, we have $\operatorname{Re} z > 4.7 - \ln\lambda - .005\mu_0$ for z in this disk, so the derivative is now greater than $\lambda e^{4.7 - \ln\lambda - .005\mu_0}$. By applying the expansion theorem again, we now have a disk of radius $.005\mu_0\mu_1$, or $.005\mu_0\lambda e^{4.7-\ln\lambda-\mu_0} = .005\mu_0 e^{4.7-\mu_0}$ about z_2. Our task will be to show that $.005\mu_0\mu_1 > 1.6$, so that we may conclude that some point of $J(E_\lambda)$ is in this disk, and therefore its preimage is within .005 of the original z_0.

We begin with $.005\mu_0\mu_1$ fully expanded:

$$.005\mu_0\mu_1 = .005\mu_0 e^{4.7-\mu_0} = .005(4.7 - \ln\lambda)e^{-.005}e^{4.7-.005(4.7-\ln\lambda)\exp(-.005)}$$

Then by noting $-4 \leq \ln\lambda \leq -1$, we can see that

$$.005\mu_0\mu_1 \quad \geq \quad .005(4.7+1)e^{4.695-.005(4.7+4)\exp(-.005)}$$

$$\begin{aligned} &= .0285e^{4.695-.0435/\exp(.005)} \\ &> .0285e^{4.6515-.0435} \\ &> .0285e^{4.6515} \end{aligned}$$

and by expanding $e^{4.65}$ in an order five Taylor series, we can now calculate that that $.005\mu_0\mu_1 > 1.9$, so we are done.

Case 3: $n \geq 3$ In the case when it takes more than two iterations before a pixel is colored, we wish to demonstrate that before the last two iterations, we must in fact have a neighborhood of radius $r = .005$ about the point z_n which is contained in the image of the original pixel.

Let $z_n = E_\lambda^n(z_0)$. We begin by noting that if $\operatorname{Re} z_n \leq 1$, we would have $\operatorname{Re} z_{n+1} = \operatorname{Re} \lambda e^{z_n} \leq \lambda e^{\operatorname{Re} z}$, and as $\lambda \leq e^{-1}$, we would necessarily have $\operatorname{Re} z_{n+1} \leq 1$ as well. Therefore, if we ever enter the half plane $\{z : \operatorname{Re} z \leq 1\}$, all future iterates remain there. This not only implies that the set of all z with $\operatorname{Re} z < 1$ is in the Fatou set, but that we will not color any point after its orbit has entered the left half plane. Therefore, we assume that $z_n = \lambda e^{z_{n-1}}$ has real part greater than one.

We consider how large the derivative must be within a distance of $r = .005$ of the point z_n. This will allow us to determine the degree of contraction or expansion taking place around the point z_n using the expansion theorem. We note that $E'_\lambda(z) = \lambda e^{\operatorname{Re} z}$, so making use of our assumption that $\operatorname{Re} \lambda e^z > 1$ and therefore $\lambda e^{\operatorname{Re} z} \geq \operatorname{Re} \lambda e^z > 1$, we have on the ball $B_r(z)$ that

$$|E'_\lambda(z)| \geq \lambda e^{\operatorname{Re} z - r} = \frac{\lambda e^{\operatorname{Re} z}}{e^r} > e^{-r}$$

Then since $e^{-.005} > .99$, we see that at each iteration the ball about z_n may only shrink by a factor of .99.

Next, we must consider how much this neighborhood is expanded again after the point begins to move away from the boundary where $\operatorname{Re} z = 1$. After all, if we are more than distance $r = .005$ away from the boundary, we see that our derivative must be greater than one on the entire neighborhood and we will expand again. (This follows from noting that $E'_\lambda(z) = E_\lambda(z)$, and that $|E_\lambda(z)| \geq 1$ if $\operatorname{Re} z \geq 1$.) We use the result from case two above, in which we showed that if z_{n+2} had real part greater than 120, then $\operatorname{Re} z_n > \ln(\ln 120 - \ln \lambda) - \ln \lambda$. Extending the argument from that case once again, we see that, for z within $r = .005$ of z_{n-1}, where $\operatorname{Re} z_{n+2} > 120$, we must have

$$|E'_\lambda(z)| \geq \lambda \exp\left(\ln\left[\ln(\ln 120 - \ln \lambda) - \ln \lambda\right] - \ln \lambda - r\right) = \frac{\ln(\ln 120 - \ln \lambda) - \ln \lambda}{e^r}$$

Using the fact that $\lambda < e^{-1}$ and that $e^{-r} = e^{-.005} > .995$, we have that the derivative around this third to last point is greater than 2.6. Since we have had at most 23 iterations up to this point, each of which has contracted the neighborhood of .005 about the point by less than .99, the total contraction is less than $.99^{23} > .7$, so we still have a neighborhood of radius

greater than $(.7)(.005) = .0035$ about the point which is from the original pixel. In the third to last iteration then, we expand this neighborhood by at least 2.6, and get a neighborhood of at least $.0091 > .005$. Therefore, we have a neighborhood $B_{.005}(z_n)$ which comes from the original pixel, and the argument for case two goes through as before. ■

Chapter 3

The Family $\lambda \tan(z)$

We will consider the computation of the Julia set for the family of functions $T_\lambda(z) = \lambda \tan(z)$ in the complex plane.

Obviously the definition of normality is not useful for computing a Julia set, so we again employ an alternate method. In the case of $T_\lambda(z)$, there are two other ways to represent the Julia set which may be helpful. As T_λ is a transcendental meromorphic function with poles which are not omitted values, $J(T_\lambda)$ is the closure of the set of all preimages of poles of all orders. We will need to make some use of this fact. More significantly, T_λ has polynomial Schwarzian derivative: $S(T_\lambda)(z) = 2$. Therefore, by Theorem 2, $J(T_\lambda)$ is also the closure of the set of all points z such that $|T_\lambda^n(z)| \to \infty$ as $n \to \infty$. We will use this fact in an algorithm for computing an approximation to the Julia set of T_λ.

In computing a Julia set numerically, we proceed as before: we pick a window W, a real bound B, a pixel width d, and a bound on iterations N. We divide the region W into pixels of width d. For the midpoint z_0 of each square we compute $f^n(z_0)$ for $1 \leq n \leq N$, now checking at each stage to see if $|T_\lambda^n(z_0)| > B$. If $|T_\lambda^n(z_0)| > B$ for some $n \leq N$, we conclude that this point is indeed tending toward infinity under iteration and consider the pixel to be in the Julia set $J(T_\lambda)$. We then color the entire pixel and move on to the next pixel. If there is no $n \leq N$ such that $|T_\lambda^n(z_0)| > B$, we conclude that the pixel is in the complement of the Julia set (the Fatou set), and we do not color the pixel. The set of colored pixels again forms what we will call the computed Julia set $J_c(T_\lambda)$.

It should be clear that the Julia set and the computed Julia set for T_λ will be different. (Of course, one obvious difference is that the Julia set is defined in terms of points rather than pixels.) As before, we wish to consider whether the computed Julia set is accurate; i.e., for any pixel which we have colored, must there be a point in the pixel which is in $J(T_\lambda)$? As before, it is also possible that we have *not* colored some pixels which contain parts of the Julia set. It could be, for example, that the point we are iterating is not moving toward infinity fast enough to pass our bound in only N iterations, or that we have chosen a point

(such as a repelling fixed point) in $J(T_\lambda)$ which does not tend to infinity.

We will show that $J_c(T_\lambda)$ is accurate for positive real λ for some reasonable choices of N, B, and d. The proofs we use would however generalize easily to the case of negative real λ, allowing us to conclude that the computed Julia sets will be accurate for all real λ.

3.1 Mapping Properties of $\lambda \tan(z)$

We will require some description of how $\lambda \tan(z)$ maps the complex plane. We begin by noting that we can write $T_\lambda(z) = \lambda \tan(z)$ as follows:

$$\lambda \tan(z) = \frac{\lambda}{i} \frac{e^{iz} - e^{-iz}}{e^{iz} + e^{-iz}} = -i\lambda \frac{e^{2iz} - 1}{e^{2iz} + 1}$$

Therefore, we can represent $T_\lambda(z)$ as the composition $-i\lambda L(\exp(2iz))$ where $L(z)$ is the Möbius transformation

$$L(z) = \frac{z-1}{z+1}$$

We consider the mapping of vertical and horizontal lines and strips under the map $\tan(z) = -iL(\exp(2iz))$. We will return to the general case for $\lambda \tan(z)$ after we have first discussed the specific case where $\lambda = 1$, noting that the only difference will be in a dilation and rotation after the mapping resulting from $\tan(z)$. If we start with a horizontal line $z = x + iy_0$ with imaginary part y_0, then under the map $\exp(2iz)$ we get $\exp(2i(x + iy_0)) = \exp(-2y_0 + 2ix) = \exp(-2y_0)[\cos(x) + i\sin(x)]$, so this horizontal line is mapped to a circle C_a of radius $a = \exp(-2y_0)$ centered at the origin. The circle C_a is then mapped by the Möbius transformation $-iL(z)$ to some circle (or line). We can specify the Möbius transformation by its behavior at three points. Under the map $-iL(z)$ the points a, $-a$, and ai on C_a are mapped as follows:

$$-iL(a) = i\frac{1-a}{1+a} \tag{3.1}$$

$$-iL(-a) = i\frac{1+a}{1-a} \tag{3.2}$$

$$-iL(ai) = i\frac{1-ai}{1+ai} \tag{3.3}$$

(We note that for $a \neq 1$, points (3.1) and (3.2) above are strictly imaginary.) If we consider the horizontal line that is the real axis (where $y_0 = 0$), then we have that $a = 1$, so these points map to 0, 1, and ∞. Thus, (not surprisingly) the real axis maps onto itself under $\tan(z)$. We note that in general $-iL(ae^{i\theta}) = \infty$ only if $|a| = 1$, so for $y_0 \neq 0$, infinity is not a point on the image curve. Thus the horizontal line with imaginary part y_0 mapped to a circle if $y_0 \neq 0$. Then we note that $iL(\overline{z}) = i\overline{L(z)}$, so by symmetry we must have a circle

centered on the imaginary axis. As a result, the purely imaginary points (3.1) and (3.2) must be the top and bottom points of the circle; that is, the points with the maximum and minimum imaginary parts. Since the real axis maps to itself, horizontal lines with imaginary part $y_0 \neq 0$ map to circles centered on the imaginary axis and lying either entirely above or entirely below the real axis. (See figure 3.1.)

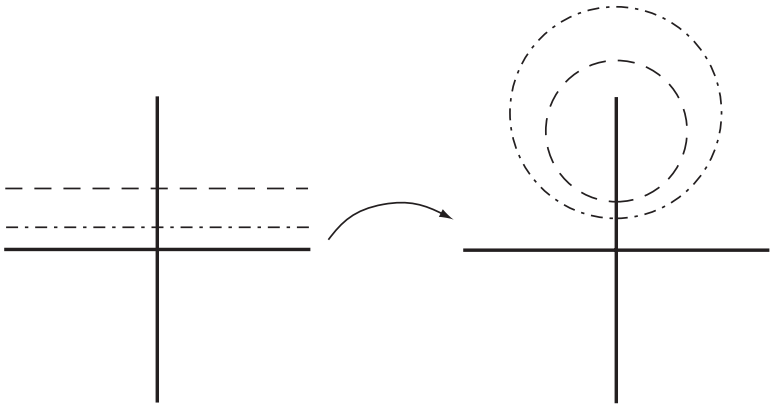

Figure 3.1: Horizontal lines map to circles centered on the imaginary axis, and on the same side of the real axis.

The radius ρ of the image circle $-iL(C_a)$ can now be calculated. It is one half the distance between the two points (3.1) and (3.2):

$$\rho = \frac{1}{2}\left(\frac{1+a}{1-a} - \frac{1-a}{1+a}\right) = \frac{2a}{1-a^2} = \frac{2e^{-2y}}{1-e^{-4y}} \tag{3.4}$$

(The above assumes that point (3.1) is closer to the origin than point (3.2), i.e., that $y > 0$. If $y < 0$, the radius is the negative of this quantity.) The center of the circle is at a point ic halfway in between (3.1) and (3.2):

$$ic = \frac{1}{2}\left[L(a) + L(-a)\right] = i\frac{a^2+1}{a^2-1} = i\frac{e^{-4y}+1}{e^{-4y}-1} \tag{3.5}$$

If $y_0 > 0$, then $\exp(2iz)$ maps the horizontal line with fixed imaginary part y_0 to a circle C_a of radius $a = \exp(-2y_0) < 1$. This intermediate circle is then mapped by $-iL(z)$ to a circle above the real axis, which intersects the imaginary axis at points above and below i. (Consider the location of points (3.1), (3.2), and (3.3) above. All are above the real axis, and (3.1) and (3.2) are above and below i respectively.) Conversely, if $y_0 < 0$, the intermediate circle has radius $a \geq 1$, and the image of $x + iy_0$ under $\tan z$ is a circle below the real axis and which contains $-i$. As $y_0 \to \infty$, the image circles contract about i, and as $y_0 \to -\infty$, the image circles contract about $-i$.

Therefore, horizontal strips can map to three different types of regions. If the strip lies entirely above the real axis, then it maps to the region between two nested, non-intersecting

circles containing i in the upper half-plane, and similarly containing $-i$ in the lower half-plane if the strip is entirely below the real axis. The circles are not centered on the same point, and thus form an off-center annulus. (See figure 3.2.) If the strip goes from the real

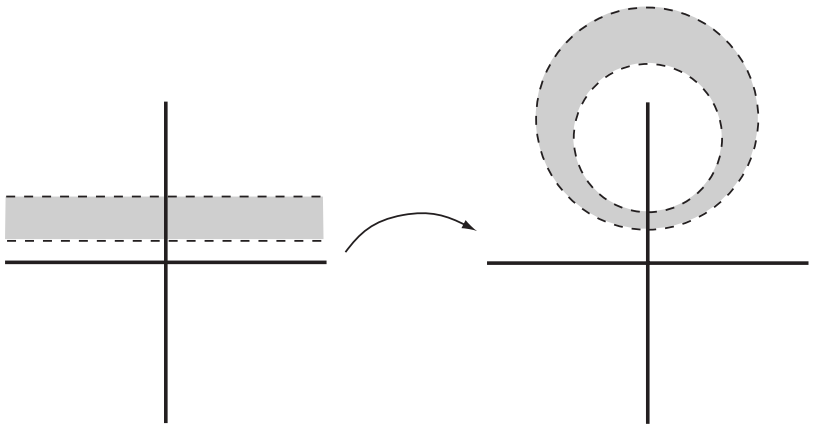

Figure 3.2: Horizontal strips map to off-center annuli.

axis to part of the upper or lower half planes, then it maps to the same half plane less a disk about the point i or $-i$. (See figure 3.3.) Finally, if the strip crosses the real axis, it

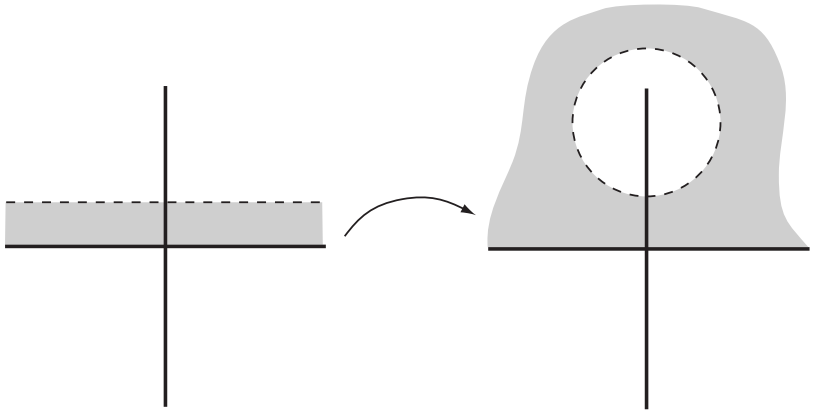

Figure 3.3: Horizontal strips including the real axis map to the half-plane less a disk.

maps to the entire complex plane less two disks, one containing i and one containing $-i$. (See figure 3.4.) In the case where the horizontal strip is the entire complex plane, the strip is mapped to the entire complex plane less the points $\pm i$, which are the only omitted values for $\tan(z)$.

Next, we consider vertical lines, which are of the form $z = x_0 + iy$ with x_0 fixed. These lines are mapped by $\exp(2iz)$ to rays from 0 to ∞ which make an angle of $2x_0$ with the real axis. (See figure 3.5.) As $y \to \infty$, the ray approaches 0, and as $y \to -\infty$ the ray approaches ∞. Pretend for a moment that this ray is an entire line; we can describe the

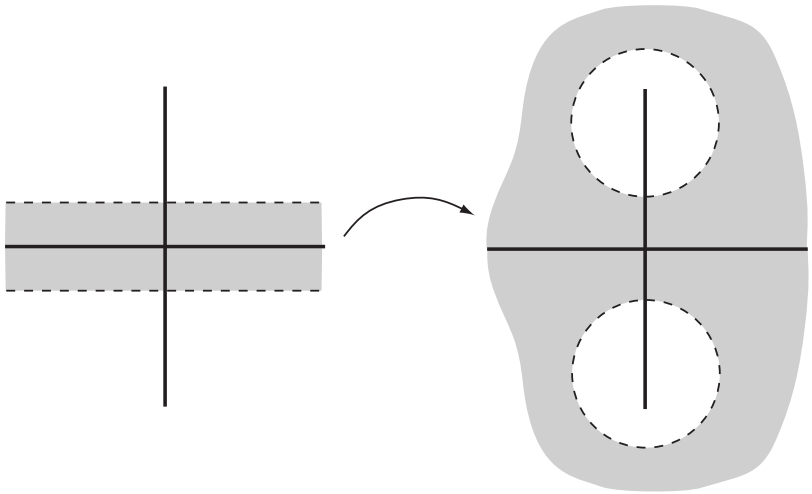

Figure 3.4: Horizontal strips across the real axis map to the plane less two disks.

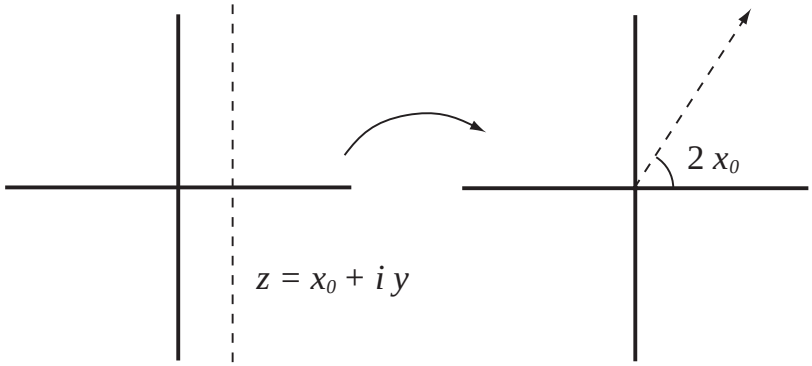

Figure 3.5: Vertical lines $z = x_0 + iy$ map under $\exp(2iz)$ to a ray which makes an angle $2x_0$ with the real axis.

Möbius transformation $-iL(z)$ by considering its action on the three points 0, ∞, and $\exp(2ix_0)$. These points are mapped to the points i, $-i$, and $\tan(x_0)$, respectively. (The point $x + 0i$ is mapped to $\exp(2ix)$, but $\tan(x + 0\,i) = \tan(x)$.) These three points form a straight line rather than a circle in only two cases: if $\tan(x) = 0$, which means that $x = n\pi$, or if $\tan(x) = \infty$, which means that $x = (2n + 1)\pi/2$. In the other cases, since we have only the ray from 0 (as $y \to \infty$) to ∞ (as $y \to \infty$) mapped under $L(z)$, the arc of the image circle stretches from i (as $y \to \infty$), through $\tan(x)$, and approaching $-i$ (as $y \to -\infty$). (See figure 3.6.) When $x = n\pi$, the point $\tan(x) = 0$ forms the third point on the image line and we get the line segment between i and $-i$ on the imaginary axis. When $x = (2n + 1)\pi/2$, we have $\tan(x) = \infty$, so the third point is at ∞ and we get the line segment joining i to $-i$ by passing through ∞ on the imaginary axis.

Therefore there are four types of regions that an infinite vertical strip can map to. Vertical strips that do not include a real value of $(2n + 1)\pi/2$ or $n\pi$ (n an integer) are mapped to

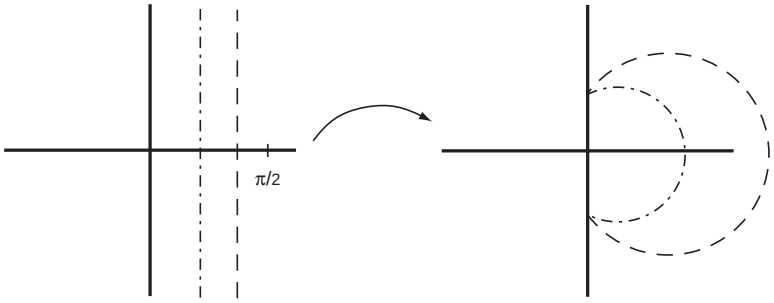

Figure 3.6: Vertical lines map to arcs of circles between $\pm i$.

crescents stretching from i to $-i$. (See figure 3.7.) Vertical strips which cross a multiple

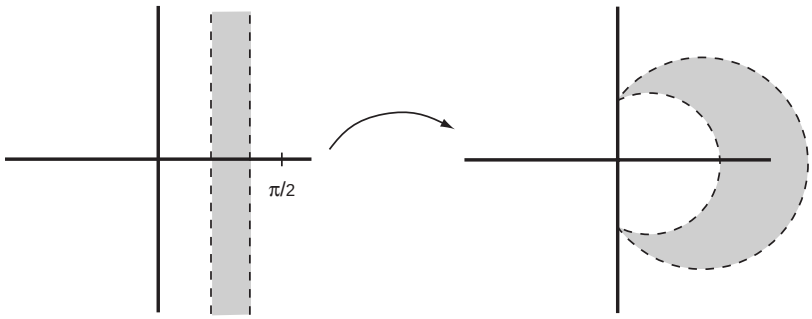

Figure 3.7: Vertical strips with real part not including a multiple of $\pi/2$ map to crescents connecting $-i$ to i.

of π map to the interior of a region bounded by parts of two circles to the left and right of the imaginary axis which meet at $\pm i$. (See figure 3.8.) Vertical strips which include a real number of the form $(2n+1)\pi/2$ are mapped to the exterior of two such circles. (See figure 3.9.) Strips which cover both kinds of real values are mapped onto the entire complex plane less the points $\pm i$. (The function $\tan(z)$ is π-periodic, so if we have a vertical strip wider than π, then we have hit everything except for the omitted values.)

Finally, if we consider rectangular regions of the plane, we have the intersection of a horizontal and vertical strip. The pixels we are interested in are such rectangular regions. We get different types of image shapes for a box under the map $\tan(z)$ depending on whether or not the box crosses a vertical line of the form $\operatorname{Re} z = n\pi$, a line of the form $\operatorname{Re} z = (2n+1)\pi/2$, or the real axis. Figures 3.10, 3.11, 3.12 and 3.13 show some of the possibilities.

When we deal with the function $T_\lambda(z)$ with $\lambda \neq 1$, we have to include a dilation and rotation as well. Under these circumstances, we get the following results:

A horizontal line with imaginary part y_0 is mapped to a circle with center and radius given by

$$\lambda ic = \lambda i \frac{1+e^{-4y_0}}{1-e^{-4y_0}}, \qquad \lambda\rho = \frac{2\lambda e^{-2y_0}}{1-e^{-4y_0}}$$

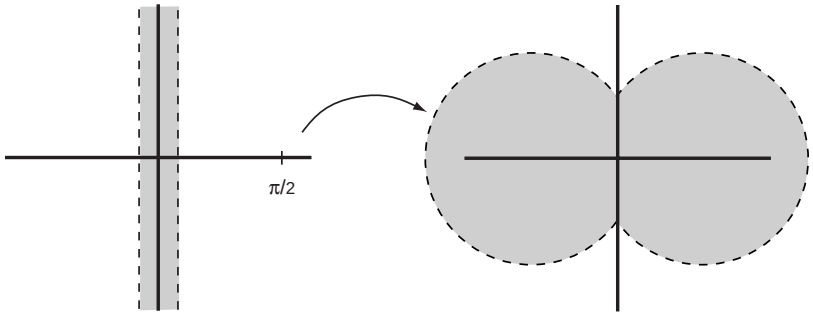

Figure 3.8: Vertical strips crossing a real multiple of π map to a region bounded by two circles meeting at $\pm i$.

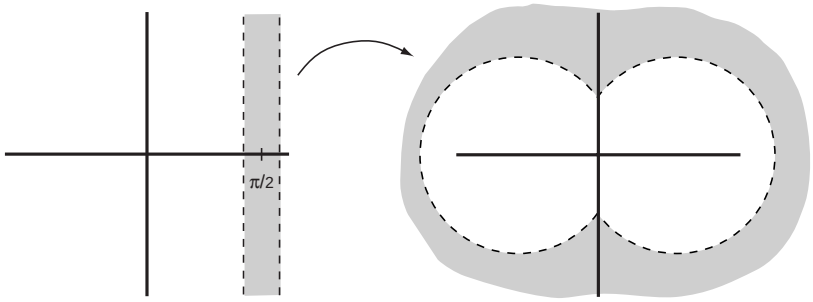

Figure 3.9: Vertical strips crossing a pole map to the exterior of a region bounded by two circles meeting at $\pm i$.

respectively. (Again, the radius may need to be adjusted for sign.)

A vertical line with real part x_0 goes to a piece of a circle symmetric with respect to the real axis connecting $\pm\lambda\, i$ and going through $\lambda \tan(x_0)$. Of course, when $\lambda = 1$, the above correspond to our previous results.

3.2 Julia sets for λtan(z)

We now discuss a few properties of the Julia sets for the family $\lambda \tan(z)$, focusing primarily on the case where λ is real.

First note that if λ is real and positive, the mapping properties of the previous section show that the upper half plane maps to the upper half plane, and the lower half plane to the lower half plane. Therefore we see by Montel's theorem that the family T_λ^n is normal in these regions. If $\lambda < 0$, the upper and lower half-planes map to each other, but both still miss the real axis, and therefore by Montel's theorem are in the Fatou set. Therefore, for real λ, the Julia set must be contained in the real line. We will not in general give further consideration to the case where $\lambda < 0$, and assume we are working with positive λ.

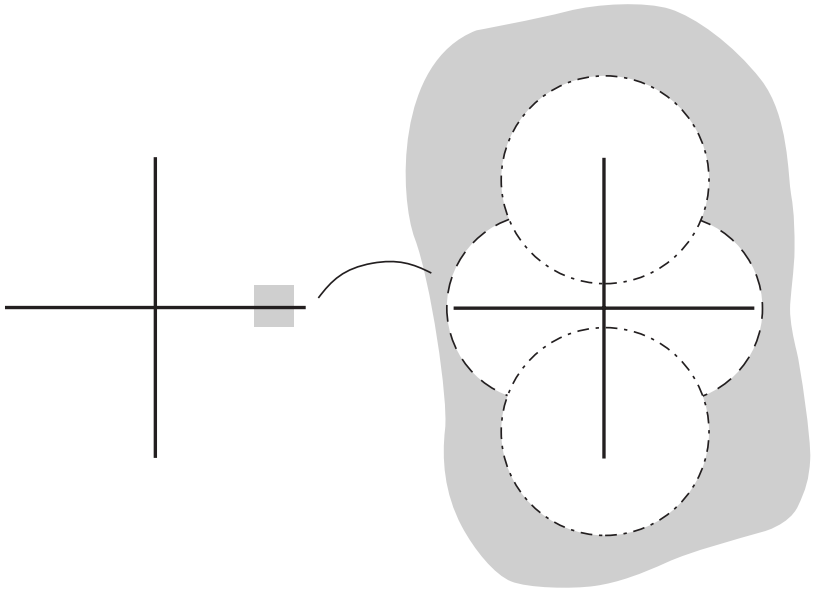

Figure 3.10: A pixel which contains a pole.

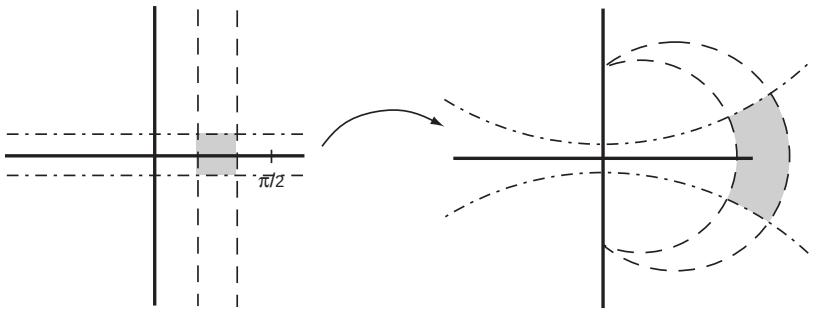

Figure 3.11: A pixel crossing the real axis.

If $\lambda > 1$, then we see that $T'_\lambda(x) = \lambda \sec^2(x) \geq \lambda > 1$ for all real x. So for $\lambda > 1$, we can assure that the derivative of $T_\lambda(z)$ will be strictly greater than one for z real. At each iteration, the interval therefore expands by a given amount. Eventually, an interval of any size will therefore be expanded to a length greater than π, which implies that the interval is now covering a pole. Therefore we have shown that if $\lambda > 1$, we have the preimage of a pole in every neighborhood of any real point. Since the preimages of the poles are in the Julia set, we have shown that every real point is in the closure of the Julia set, and hence, that the entire real line is contained in $J(T_\lambda)$. The same argument holds when $\lambda = 1$, with the exception that we may need to excise a small region surrounding any multiple of π that the image of the pixel may include; at this point, the derivative is only 1. So for $\lambda \geq 1$, the Julia set is the real line.

For $|\lambda| < 1$, the Julia set is less simple. We note that 0 is now an attracting fixed point, and hence a neighborhood about 0 is contained in the Fatou set. Similarly, a neighborhood

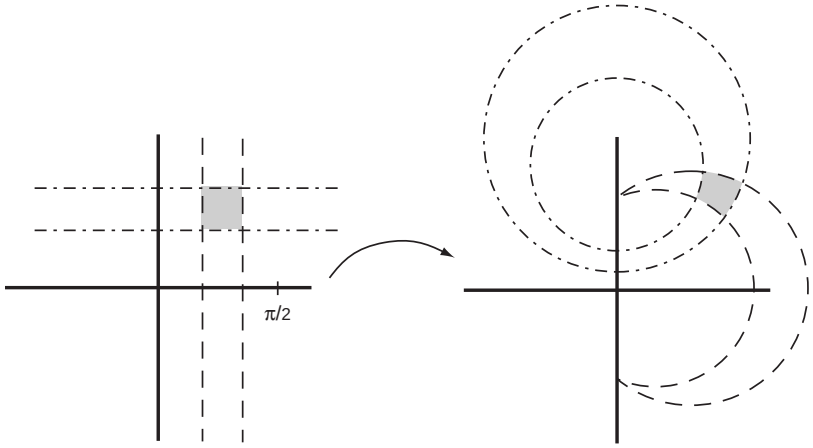

Figure 3.12: A pixel off the real axis and with real parts away from poles and multiples of π.

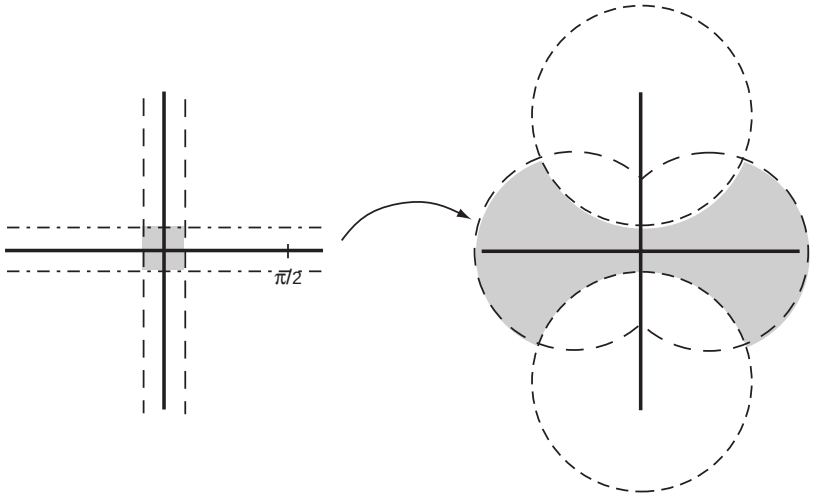

Figure 3.13: A pixel containing the origin.

around all multiples of π must be in $F(T_\lambda)$. By invariance, we must also include all preimages of these neighborhoods in the Fatou set. This recursive excising of intervals is reminiscent of the construction of a Cantor set. In fact, Devaney and Keen showed [11] that the Julia set for T_λ where $\lambda < 1$ is a Cantor set in the real line, and that iteration of T_λ is equivalent to a shift map on infinitely many symbols.

The asymptotic values of T_λ play a role in determining the Fatou set. An asymptotic value for a function f is a value v for which there exists a path $\sigma(t)$, $t \in [0, 1)$, with $\sigma(t) \to \infty$ as $t \to 1$, such that $f(\sigma(t)) \to v$ as $t \to 1$. (In other words, $f(z)$ approaches v as z tends to infinity along σ.) From our mapping properties, we see immediately that $\pm\lambda\, i$ are asymptotic values for T_λ, and that they are in fact the only asymptotic values. Alternatively, we could note that the omitted values of meromorphic functions are also asymptotic values. (See

for example [17, p. 199].) Then from the theorem of Nevanlinna mentioned earlier, since T_λ has constant Schwarzian derivative, there are exactly two asymptotic values. So these asymptotic values are the only ones.

There are no wandering domains and no Baker domains for this family (as it has polynomial Schwarzian derivative). Since there are no critical values, each component of the Fatou set of T_λ must either contain an asymptotic value or attract the infinite forward orbit of such a value. Keen and Kotus observed [19] that this implies that if the asymptotic values are also preimages of poles, the Julia set must be the entire plane. (If the asymptotic values are preimages of poles, they are in the Julia set and have a finite forward orbit.) This cannot happen to T_λ for real λ, as $\pm\lambda i$ are the asymptotic values and all preimages of the poles of $\lambda \tan(z)$ are real if λ is. However, we do note that both the upper and lower half plane contain an asymptotic value for real λ.

3.3 Accuracy of Computed Julia Sets for tan(z)

We now consider the accuracy of the computed Julia set of $T_\lambda(z)$ for $\lambda = 1$. We will show that if the Julia set is computed using $N = 50$, $B = 210$, and $d = .01$, then the Julia set is accurate. (We will often refer to the radius $r = .005$ of the pixels of width $d = .01$.) The values of N and d were chosen somewhat arbitrarily, but are of reasonable magnitude. The value of our bound B was chosen large enough to make the analysis which follows work, although it too is within the realm of "reasonable" choices. However, we will also see that with a modified algorithm, we can establish accuracy with a bound of only 110. We will not need to actually give thought to our window W with the family T_λ, so long as we do not check for $|z| > B$ until after we have performed one iteration. (If we check the modulus before one iteration, we will of course have to restrict W to lie entirely within a radius of 210 from the origin.) In the imaginary direction, it is clear that any point with large imaginary part is mapped close to one of the asymptotic values, and so will not be colored. In the discussion of accuracy, we will see that there are no restrictions on W required. Of course $\tan(z)$ is periodic, so a window of width π will show all the same dynamics that a larger window would show. In our analysis, then, we will usually restrict ourselves to considering the region with real part between 0 and π for simplicity.

We first develop bounds on the real and imaginary part of a point in order for it to be mapped under T_λ to a point with modulus greater than $B = 210$. Vertical lines with fixed real part x_0 we already know are mapped to arcs of circles symmetric with respect to the real axis and passing through $\tan(x_0)$. Therefore, $|\tan(x_0)|$ is an upper bound for $|\tan(x_0 + iy)|$, so long as $|\tan(x_0)| > 1$. (See figure 3.14.) If $|\tan(x_0)| < 1$, then it is clear that this edge of the circle is closer to the origin than are the asymptotic values $\pm i$. However, in this case it is also clear that $|\tan(x_0 + iy)| < 210$.

Now we know that tangent has a pole at the point $\pi/2 \approx 1.5708$, and on the real axis

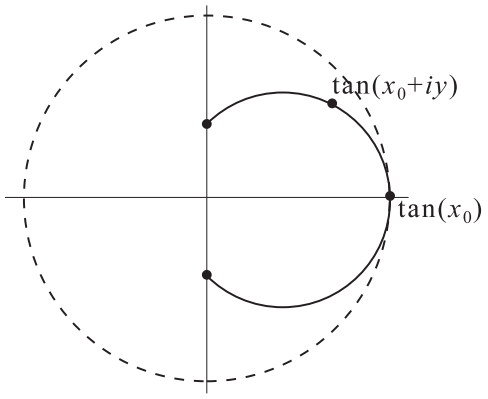

Figure 3.14: $|\tan(x_0)| \geq |\tan(x_0 + iy)|$, if $|\tan(x_0)| \geq 1$.

$|\tan(x)|$ is increasing for points near but to the left of $\pi/2$ and decreasing for points near but to the right of $\pi/2$. (Note that $\tan(x)$ is always increasing, but that $\tan(x)$ is negative on $(\pi/2, \pi)$, so $|\tan(x)|$ is *decreasing* here.) Since we can compute that $|\tan(1.576)| < 210$ and $|\tan(1.566)| < 210$, we have that $|\tan(x + iy)| > 210$ implies $1.566 < x < 1.576$, or in a similar interval of the same size about another pole.

Next we attempt to bound the imaginary part of z. As we have seen, horizontal lines with imaginary part $y > 0$ map to circles above the real axis and centered on the imaginary axis. Therefore $|\tan(z)| = |\tan(x + i\,y)| < \rho + c$, where ρ and ic are the radius and center of the circles, as was given in equations (3.4) and (3.5) from section 3.1. Therefore, if we assume that the imaginary part of some point z_0 is greater than .005 in magnitude, then by the mapping properties of tangent which were developed earlier, $\tan(z_0)$ is contained in a disk of radius $2e^{(-2)(.005)}/(1 - e^{(-4)(.005)})$, or $2e^{.01}/(e^{.02} - 1) < 105$, and centered at $(1 + e^{-.02})/(1 - e^{-.02})$, which is less than 105. (The estimates can be obtained by using a Taylor series for e^x; we can compute using only the first two terms of the series that $1.0094 \leq e^{.01} \leq 1.0106$ and $1.0194 \leq e^{.02} \leq 1.0206$.) In the first iteration, a point with imaginary part more than .005 away from the real axis is mapped within this circle, and the modulus of the point is less than 210.

Therefore, we can conclude that the only points which can be mapped into the region where $|z| > 210$ in one iteration are those points inside a square with side of length .01 centered on the real axis and containing a pole of $\tan(z)$. This is fine so far, because we know that the entire real line is the Julia set for $\tan(z)$, and no point in this box is any further away from the real axis than .005. Therefore any pixel of radius $r = .005$ whose center is mapped to a point with real part greater than 210 must have that center in the interior of one of these boxes, and therefore the pixel must contain a point of the real axis. This point is of course in the Julia set. Now we need only determine that anything which maps into this box in the remaining 49 iterations is within .005 of a point in the Julia set. (In other words, it is within .005 of the real axis.)

We use the following lemma for the more general function $\lambda \tan(z)$, where $\lambda > 0$:

Lemma 2 *Given $\lambda > 0$ and a region $R = \{z : x_0 \leq \operatorname{Re} z \leq x_1, |\operatorname{Im} z| \leq y_0\}$ in the complex plane, we wish to choose x_0', x_1', and y_0' so that $\lambda \tan(z)$ maps the region $[x_0', x_1'] \times [-y_0', y_0']$ onto R. This can be done if x_0', x_1', and y_0' are chosen as follows:*

$$x_0' = \arctan(x_0/\lambda) \tag{3.6}$$

$$x_1' = \arctan\left(\frac{x_1^2 + y_0^2 - \lambda^2 + \sqrt{4\lambda^2 x_1^2 + (x_1^2 + y_0^2 - \lambda^2)^2}}{2x_1}\right) \tag{3.7}$$

$$y_0' = \frac{1}{4}\ln\left(\frac{\lambda^2 + x_0^2 + 2\lambda\, y_0 + y_0^2}{\lambda^2 + x_0^2 - 2\lambda\, y_0 + y_0^2}\right) \tag{3.8}$$

Proof: We know that a vertical line with real part x_0' will be mapped to the arc of a circle connecting $\pm\lambda\, i$ through the point $\lambda \tan(x_0')$. Since $|\lambda \tan(x_0')|$ is an upper bound for $|\operatorname{Re}(\lambda \tan(x_0' + iy))|$ (see figure 3.14 again), we get that $\arctan(x_0/\lambda)$ will suffice for x_0'.

Getting x_1' is more difficult. We note that we need to enclose an entire box, but that the vertical line with real part x_1' is mapped to a circle with center c and radius r which reaches out to $\lambda \tan(x_1')$ at its furthest. Thus, we need to determine how far out $\lambda \tan(x_1')$ needs to be in order for the resulting circle to completely enclose the box. We will call this point d and refer to figure 3.15. (Our concern here is to avoid clipping off the corners of the box.)

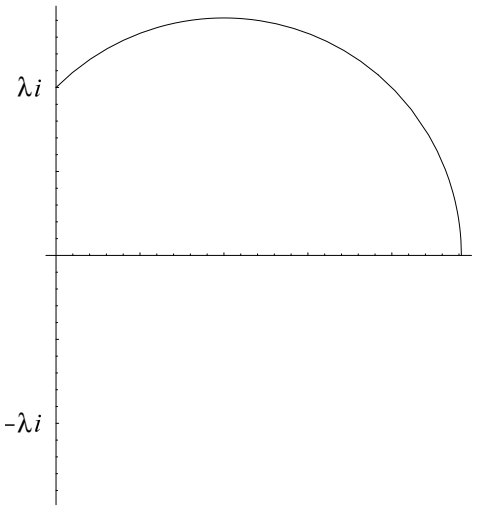

Figure 3.15: The outer circle used in covering a given box

We note that

$$x_1 = c + \sqrt{r^2 - y_0^2}$$

and so

$$\begin{aligned} d &= c + r \\ &= \left(x_1 - \sqrt{r^2 - y_0^2}\right) + r \end{aligned} \tag{3.9}$$

We now need to determine the center c and radius r of the circle. The circle goes through the three points $(d, 0)$, $(0, \pm\lambda)$ in the Cartesian plane. To determine the center, we will find the point where the perpendicular bisectors of two chords meet. The two points $\pm\lambda\, i$ give a chord on the imaginary axis, so one perpendicular bisector is the real axis. Another is found by looking at the chord from λi to d. Working in the real cartesian plane, these are the points $(0, \lambda)$ and $(d, 0)$, so we see that the chord has slope $-\lambda/d$ and midpoint $(d/2, \lambda/2)$. Therefore the perpendicular bisector is $y = (d/\lambda)x - d^2/(2\lambda) + \lambda/2$. So the center of the circle is where this line and the line $y = 0$ (the real axis) cross, which is

$$c = \frac{d}{2} - \frac{\lambda^2}{2d}$$

The radius can be obtained by subtracting the center point from d:

$$r = d - \left(\frac{d}{2} - \frac{\lambda^2}{2d}\right) = \frac{d}{2} + \frac{\lambda^2}{2d}$$

So in the end, by plugging into equation (3.9) above, we have

$$d = x_1 + \frac{d}{2} + \frac{\lambda^2}{2d} - \sqrt{\left(\frac{d}{2} + \frac{\lambda^2}{2d}\right)^2 - y_0^2}$$

and solving for d yields

$$d = \frac{x_1^2 + y_0^2 - \lambda^2 + \sqrt{4\lambda^2 x_1^2 + \left(x_1^2 + y_0^2 - \lambda^2\right)^2}}{2x_1}$$

This leads to a choice of x_1' as given in the lemma.

Finally we wish to know how small the imaginary part needs to be in order to hit the given region. We know that a horizontal line with imaginary part $y > 0$ goes to a circle centered on the imaginary axis and above the real axis, and that smaller values of y result in larger circles. Therefore we want to find y_0' such that the circle given by $\lambda \tan(x + y_0')$ for $-\frac{\pi}{2} \le x \le \frac{\pi}{2}$ just touches the upper left hand corner of the rectangle. We want the distance from the center of the circle (at $(0, c)$) to the corner of the rectangle (at (x_0, y_0)) to be the radius of the circle. Using the values we have for the point c and for the radius ρ of this circle from equations (3.5) and (3.4) from section 3.1, we must therefore solve

$$\rho = \frac{2\lambda e^{-2y}}{1 - e^{-4y}} = \sqrt{x_0^2 + (c - y_0)^2} = \sqrt{x_0^2 + \left(\lambda \frac{1 + e^{-4y}}{1 - e^{-4y}} - y_0\right)}$$

for y. Doing so we obtain

$$y = \frac{1}{4} \ln \left(\frac{\lambda^2 + x_0^2 + 2\lambda\, y_0 + y_0^2}{\lambda^2 + x_0^2 - 2\lambda\, y_0 + y_0^2} \right)$$

This yields the choice of y_1' as given in the lemma. ■

We apply the lemma repeatedly. We start with the box about $\pi/2$. At each stage, we will find a rectangular box which will map onto the current box under the map $\tan(z)$. We note that the formulas for x_0' and x_1' are decreasing, always positive (for positive values of x_0 and x_1), and $x_0' < x_1'$. So the box moves backwards towards zero along the real axis. Similarly, we also have boxes that move toward the origin if we start with the box about $-\pi/2$. If we start with a box around a pole of greater magnitude, we see that in the first preimage, we get a box in the interval $(-\pi/2, \pi/2)$ and with a real part slightly larger in magnitude than if we had started with the box around $\pm\pi/2$. Thus in all cases, we will be moving towards the origin in the interval $(-\pi/2, \pi/2)$ when back iterating.

The derivative of y_0' with respect to x is

$$\frac{-2\, x\, y}{\left(x^2 + (-1+y)^2\right)\left(x^2 + (1+y)^2\right)}$$

and the derivative of y_0' with respect to y is

$$\frac{1 + x^2 - y^2}{\left(x^2 + (-1+y)^2\right)\left(x^2 + (1+y)^2\right)}$$

The first is negative and the second is positive if we assume x and y are positive, and that $y < 1$. We will show that in the region $(.17, 1.57) \times (0, .005)$, the y value stays less than .005. We use .17 for the left hand limit because the arctangent iterated on the point 1.56 fifty times is greater than .17, hence in fifty iterations, the x coordinate of our box cannot have moved past this point. (See Appendix A.) From the derivatives, we see that the largest value we could obtain for y_0' in equation (3.8) above using x and y within such a box occurs at the upper left hand corner, and at this point, $y_0' \approx 0.00486$, which is less than .005. We see that choices of x and y coordinates in this box result in another y coordinate within this box. Therefore as we back iterate, each box that we have is symmetric about the real axis and the edge of the box is less than $r = .005$ away from the real axis. Therefore every pixel which has a center sent into the boxes about the poles of $\tan(z)$ in fifty or fewer iterations is within .005 of the real axis, and therefore contains a part of the Julia set. We have proved the following:

Theorem 5 *The computed Julia set for* $\tan(z)$ *with pixel radius* $r = .005$*, bound* $B = 210$*, and maximum iterations* $N = 50$ *is accurate.*

We will make one further observation: Given that points with moderately large imaginary part are mapped to a small circle enclosing one of $\pm i$, it is clear that points which go to infinity must do so by having the real part become large. In other words, we could adjust our algorithm to look for points z such that the real part of their n^{th} image under $\tan(z)$ becomes large, i.e., that $|\mathrm{Re}\, z_n| > B$. (In fact, we shall devote some time in the case where $\lambda < 1$ to showing that any colored pixel in fact has a point which goes toward infinity in the real direction.) Using such a modified algorithm, we can in fact show that a bound of $B = 110$ will give an accurate representation. We will give only a brief summary of how the above work would need to be altered for this algorithm.

Since $|\tan(x)| \geq |\mathrm{Re}\, \tan(x+iy)|$, then $|\tan(x)|$ could still be used as bound to control $|\mathrm{Re}\, \tan(x+iy)|$. Now we see that the real part of point x such that $|\mathrm{Re}\, \tan(x+iy)| > 110$ must be between 1.56 and 1.58. For the restriction on the imaginary part, note that again the line $x + i\, y_0$ is mapped to a circle of radius ρ and center c as given before. The radius of such a circle is an upper bound on its real part, so we have that if $y \geq y_0 > 0$, then

$$|\mathrm{Re}\, \tan(x+iy)| \leq \frac{2e^{-2y_0}}{1-e^{-4y_0}}$$

If we are looking in general for where $|\mathrm{Re}\, \tan(z)| = B$, we can solve this to find $e^{-2y} = 1+\sqrt{1+B^2}$, or $y = -\frac{1}{2}\ln(\sqrt{1+B^2}-1) - \ln(B)$. So we know that if $|\mathrm{Re}\, \tan(z_0)| \geq B$, then

$$|\mathrm{Im}\,(z_0)| \leq -\frac{1}{2}\left[\ln\left(\sqrt{1+B^2}-1\right) - \ln(B)\right]$$

With $B = 110$, this becomes

$$|\mathrm{Im}\,(z_0)| \leq -\frac{1}{2}\left[\ln\left(\sqrt{1+110^2}-1\right) - \ln(110)\right] \approx .0045 < .005$$

Thus, we have as before that the imaginary part must be no further than $r = .005$ away from the real axis for the point to be mapped to a point with real part greater than 110. The rest of the proof proceeds as before, finding all the preimages of boxes that map into the rectangle $[1.56, 1.58] \times [-.005, .005]$.

We shall not deal with this modified algorithm again, although it would simplify some of our later work.

3.4 Accuracy of Julia Sets for $\lambda > 1$

We will use the same analysis as used in the case where $\lambda = 1$ above. We will keep $r = .005$ and $N = 50$, but we will now use $B = 210\lambda$. Such a choice allows us to use an almost identical analysis as we used when discussing $\tan(z)$: we have the same bounds as before for a point z_0 to be mapped to $z_1 = \lambda \tan(z)$ with $|z_1| > B$, namely that $1.566 < \mathrm{Re}\, z_0 < 1.576$ and $|\mathrm{Im}\, z_0| < .005$, or z is in a similar box around any pole of $\tan(z)$.

In addition, if we continued to work with the fixed $B = 210$, then it is clear that for larger values of λ that $J_c(T_\lambda)$ would *not* be accurate. For example, if we consider $\lambda > 210$, we see that the region where $\tan(z)$ is sufficiently close to 1 (which includes any point with sufficiently large imaginary part) would be found to be in the Julia set, even though such points are clearly not going to infinity. We might therefore reasonably be inclined to scale the bound for large λ when computing Julia sets even if we were not establishing the accuracy of the representation, since we are trying to measure whether or not a point is tending toward infinity. If we are judging whether a point is tending to infinity by how large it becomes, "large" is clearly a relative term.

We can now proceed as in the case where $\lambda = 1$, by finding a sequence of boxes which map into the region $[1.566, 1.576] \times [-.005, .005]$ under $\lambda \tan(z)$ in somewhere between one and forty-nine iterations. As we back iterate, we can again use the formulas in Lemma 2 to determine the boxes which are ultimately mapped to a z where $|\mathrm{Re}\, z| > B$.

As before, the real bounds x_0' and x_1' are moving towards the origin. (In fact it is clear that $|\arctan(x/\lambda)| < |\arctan(x)|$ if $\lambda > 1$.) However, the fiftieth preimage of $x = 1.566$ is now more difficult to determine. In fact, as $\lambda \to \infty$, $T_\lambda^{-50}(1.56) \to 0$.

We do know that as before our function determining the height of the box is increasing in y and decreasing in x. Also, the derivative of our expression for y_0' with respect to λ is

$$\frac{y_0\ (-\lambda^2 + {x_0}^2 + {y_0}^2)}{\left({x_0}^2 + (\lambda - y_0)^2\right)\ \left({x_0}^2 + (\lambda + y_0)^2\right)}$$

and for small values of x and y this is negative, so the function is decreasing in λ. Therefore, (so long as $x_0^2 + y_0^2 < \lambda^2$), we should choose the smallest value of λ to find the largest value of y_0'.

The best we can do in choosing a small value of x is to let $x = 0$. If we start with the assumption $y_0 < .005$ however, with $x = 0$ and $\lambda = 1$, we get a y_0'-value of .0050000417, which is larger than .005. Therefore we cannot conclude that the y coordinate of the boxes are all less than or equal to .005. However, if we restrict λ to be at least as large as 1.00001, it turns out that then if we start with $y_0 \leq .005$ and $x_0 \geq 0$, then $y_0' \leq .005$ as desired. Thus we have shown accuracy for $\lambda > 1.00001$.

Next we deal with the case where $1 < \lambda \leq 1.00001$. For any fixed λ, the largest value of y_0' still occurs at the largest value of y_0 and smallest value of x_0. Now however we *can* restrict the smallest x_0: given that $\lambda \leq 1.00001$, we can conclude that $T_\lambda^{-50}(1.566) > .17$. (See Appendix A.)

Then again using our formula for y_0', we can conclude that if $x_0 \geq .17$, $y_0 \leq .01$, and $\lambda \geq 1$, we must have

$$y_0' \leq \frac{1}{4} \ln\left(\frac{1 + .17^2 + 2(.005) + .005^2}{1 + .17^2 - 2(.005) + .005^2}\right) = \frac{1}{4} \ln\left(\frac{1.03892}{1.01892}\right) < \frac{.0195}{4} < .005$$

Therefore, points inside the block $(.17, 1.56) \times (-.005, .005)$ stay within that block for fifty iterations. We can conclude that the Julia set is accurate for $\lambda > 1$:

Theorem 6 *The computed Julia set for $\lambda \tan(z)$ with pixel radius $r = .005$, bound $B = 210\lambda$, and maximum iterations $N = 50$ is accurate for all $\lambda > 1$.*

3.5 Accuracy of Julia Sets for $0 < \lambda < 1$

The case where $\lambda \geq 1$ is in some sense uninteresting, since it is easy to show that the Julia set is the entire real line. Thus, computed pictures have limited usefulness. More interesting is the case where $\lambda < 1$, when the Julia set is a Cantor set on the real axis. In this case, locating points in the Julia set as we have before is more challenging. However, we do know that all poles are in the Julia set, and therefore, all preimages of poles. We will show that if a pixel crossing the real axis is mapped past a large bound, that the pixel in fact contains the preimage of a pole. We will also see that pixels not intersecting the real axis will not be mapped past the bound, and so will not be colored. As in the case where $\lambda \geq 1$, we will not need any restrictions on the window W so long as we perform one iteration before checking to see if a point has become large.

We will show:

Theorem 7 *For $0 < \lambda < 1$, the computed Julia set for $\lambda \tan(z)$ with pixel radius $r = .005$, bound $B = 210$, and $N = 50$ is accurate.*

Proof: We will proceed as follows: We will consider a point z_0 at the center of an arbitrary pixel of radius $r = .005$. First, we will demonstrate that if the pixel does not intersect the real axis, then $|T_\lambda^n(z_0)| \leq 210$ for all $n \leq 50$. Hence, if the pixel does not intersect the real axis, it will not be colored by our algorithm. Next, we will consider the case where the pixel does intersect the real axis, and the point z_0 escapes our bound in a single iteration, i.e., $|T_\lambda(z_0)| > 210$. Then letting $x_0 = \operatorname{Re} z_0$, we will see that the segment $[x_0 - r, x_0 + r]$ contained in the pixel about z_0 is expanded to a length of greater than π under the map T_λ, and therefore its image must intersect a pole of T_λ. Finally, we will deal with the case where z_0 requires more than one iteration to escape, so $|T_\lambda(z_0)| \leq 210$ but $|T_\lambda^n(z_0)| > 210$ for $1 < n \leq 50$. This case is somewhat more complicated, but ultimately we will show that the segment $[x_0 - r, x_0 + r]$ does in fact contain a point in $J(T_\lambda)$ (where $x_0 = \operatorname{Re} z_0$). We will show that the interval contains a point of the Julia set in two steps. First, we will show that if $|T_\lambda^n(x_0)|$ is large, then the image of $[x_0 - r, x_0 + r]$ is expanded under the maps T_λ^m, $m \leq n$. (In other words, the image of the interval intersecting the real axis gets larger at the m^{th} stage.) This will allow us to revert to the case where z_0 escapes in a single iteration, if we can show that $|T_\lambda^n(z_0)|$ being large implies $|T_\lambda^n(x_0)|$ is also large. Second, we will show that for $m \leq n$ that $\operatorname{Re} T_\lambda^{m-1}(z_0) \in [T_\lambda^{m-1}(x_0 - r), T_\lambda^{m-1}(x_0 + r)]$. This fact will allow us to

conclude that $|T_\lambda^n(x_0)|$ is large if $|T_\lambda^n(z_0)|$ is large. The proof that the interval expands at each stage will require us to find two repelling fixed points for T_λ; these fixed points are on the boundary of the attracting basin for the origin.

We begin by considering the case where the pixel of radius $r = .005$ does not intersect the real axis. We know then that $|\mathrm{Im}\, z_0| > .005$. Then by following the same argument as we used in section 3.3 for the case where $\lambda = 1$, we see that we are mapped inside a circle centered at λci with radius $\lambda\rho$ as given in equations (3.5) and (3.4) from section 3.1, so using the fact that $\lambda < 1$, we once again see that $|T_\lambda(z_0)| < 210$.

We next concern ourselves with the portion of this circle which is below the line ℓ given by $\mathrm{Im}\, z = .005$, since the portion above this line is mapped once again inside the same circle. We will first determine the points where ℓ intersects its image $T_\lambda(\ell)$. To do this, we find the distance d_λ such that the imaginary part of $T_\lambda(d_\lambda + .005i)$ is .005. (By symmetry, we know that $T_\lambda(-d_\lambda + .005i)$ also has imaginary part .005.) Using the fact that we have the line ℓ mapped to a circle of radius $\lambda\rho$ and centered at λci on the imaginary axis, we form a triangle with the points $d_\lambda + .005i$, $.005i$, and λci. (See figure 3.16.) We can then determine that $d_\lambda = \sqrt{\rho^2\lambda^2 - (c\lambda - .005)^2}$.

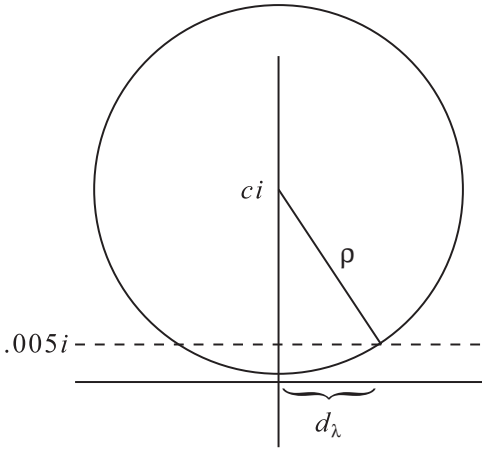

Figure 3.16: Finding the distance d_λ by forming a triangle.

We will show that if we start with real part between $\pm d_\lambda$, we cannot in fifty iterations escape past a modulus of 210. We do not need to worry about the possibility that the point escapes in the imaginary direction, because once the image of the point has imaginary part greater than .005, we know that it will be mapped inside the circle $T_\lambda(\ell)$, and the process will start again. Thus, if we escape, we do so by staying below $\mathrm{Im}\, z = .005$ and moving to the right (or left) across the plane. We wish to determine how far to the right (or left) the point can move in the remaining forty-nine iterations if we start with real part between $\pm d_\lambda$. Since $|\mathrm{Re}\, \lambda \tan(\mathrm{Re}\, z)| \geq |\mathrm{Re}\, \lambda \tan(z)|$, we will assume we have a real x between $\pm d_\lambda$, and show that this cannot move past $B = 210$ in fifty or fewer iterations.

By maximizing the quantity inside the square root for d_λ, we find that d_λ is largest when

$$\lambda = \frac{.005c}{c^2 - \rho^2}$$

(which is slightly larger than .5), and at this point, $d_\lambda = .005\rho\,(c^2 - \rho^2)^{-1/2}$ (which is slightly smaller than .5). Therefore, for any λ, we must have $d_\lambda < .5$.

Suppose then we have a real x between $\pm d_\lambda$. We note that $|.5\tan(x)| < |x|$ for $|x| \leq .5$. This means that for $\lambda \leq .5$, $|\lambda \tan(x)| < |x|$ if $|x| \leq .5$. (In other words, if we start with x within .5 of the origin and $\lambda < .5$, x only moves closer to the origin.) But $d_\lambda < .5$, so this says that $|\lambda \tan(x)| \leq |x|$ if x starts within the interval $[-d_\lambda, d_\lambda]$ and $\lambda \leq .5$. Therefore we cannot escape past $|\mathrm{Re}\, z| > 210$ in 50 iterations (or in fact at all). We are done with $\lambda < .5$.

We then note that $d_{(.5)} \approx .499992$ and $d_{(.75)}$ is slightly larger than .433, so the minimum value for d_λ on the interval $[.5, .75]$ occurs at $\lambda = .75$. So we know $.433 < d_\lambda < .5$ for λ in $[.5, .75]$. Therefore for λ in the interval, we have $|\lambda \tan(d_\lambda)| \leq d_\lambda$ because of the following:

$$.75\tan(.5) \approx .410 < .433 < d_{(.75)}$$

(Here, we are using .5 in the argument to $\tan(z)$ on the left hand side because $d_\lambda < .5$.) Hence, for λ in this interval, if $|x| < d_\lambda$, then $|\lambda \tan(x)| < d_\lambda$, so such points will remain trapped.

We can then proceed in a similar fashion, noting that for $\lambda > .51$, we have d_λ decreasing in λ. We therefore know that for $.51 \leq a \leq \lambda \leq b \leq 1$ we will have $|\lambda \tan(d_\lambda)| \leq d_\lambda$ so long as $b\tan(d_a) \leq d_b$. Using this, we see that we must have $\lambda \tan(d_\lambda) < d_\lambda$ for $\lambda \in [.75, .8]$, since

$$.8\tan(d_{(.75)}) \approx .3698 < .4000 \approx d_{(.8)}$$

We can then deal with λ in the intervals $[.8, .9]$, $[.9, .95]$, $[.95, .98]$, and $[.98, .99]$ in the same way. Thus we can now assume that if a point manages to escape from the interval $[-d_\lambda, d_\lambda]$ in fifty or fewer iterations, we must have $\lambda > .99$, which means in turn that $d_\lambda < .1$. But the fastest growth of $|T_\lambda^n(x)|$ would be when $\lambda = 1$, and iterating $\tan(z)$ forty-nine times at .1 gets only as large as approximately .122, so we cannot escape in this case either. (See Appendix A.) Thus we have shown that we cannot escape from the region with real part within $[-d_\lambda, d_\lambda]$ in fifty or fewer iterations. So combining this with our previous result that if $|\mathrm{Re}\, z| > d_\lambda$ and $|\mathrm{Im}\, z| > .005$ then z cannot escape, we see that a point cannot in fact escape to where $|z| \geq 210$ in fifty iterations unless it started out within .005 of the real axis. This concludes the first part of the proof.

We next consider the case where the pixel of radius r surrounding z_0 intersects the real axis, and $|T_\lambda(z_0)| > 210$. (In other words, z_0 escapes in a single iteration.) Let $z_0 = x_0 + iy$. We will first show that $|T_\lambda(z_0)| > 210$ implies that $|T_\lambda(x_0)| > 210$. We begin by noting that

$$|\lambda \tan(x_0 + iy)|^2 = \lambda^2 \frac{1 + e^{4y} - 2\,e^{2y}\,\cos(2x_0)}{1 + e^{4y} + 2\,e^{2y}\,\cos(2x_0)}$$

We can solve for $\cos(2x_0)$ and find that if $|\lambda \tan(z_0)| > 210^2$, then

$$\cos(2x_0) < \left(\frac{1+e^{4y}}{2e^{2y}}\right)\frac{\lambda^2 - 210^2}{\lambda^2 + 210^2} = K\frac{\lambda^2 - 210^2}{\lambda^2 + 210^2} \tag{3.10}$$

by making the definition

$$K = \left(\frac{1+e^{4y}}{2e^{2y}}\right)$$

to simplify the calculations which follow. Since we know $|y| < .005$, we have that $1 \leq K < 1.000051$. We see that $\cos(2x_0)$ must be negative and close to -1 for $|\tan(x_0 + iy)|$ to be greater than 210. This suggests that $|\tan(x_0)|$ will also be large, as for $\cos(2x_0)$ to be close to -1, we should have x_0 close to some multiple of $\pi/2$. Indeed this is the case, and we can describe how large $\tan(x_0)$ must be if $|y| < .005$ in order for $|\tan(x_0 + iy)|$ to be greater than 210. Using double angle identities for cosine, we obtain

$$|\tan(x_0)| = \sqrt{\frac{1-\cos(2x_0)}{1+\cos(2x_0)}} = \sqrt{-1 + \frac{2}{1+\cos(2x_0)}}$$

Then using the fact that $\cos(2x_0)$ is close to -1 and restricted by equation (3.10) above, we can find that

$$|\tan(x_0)| > \sqrt{\frac{44100 + 44100\,K + \lambda^2 - K\,\lambda^2}{44100 - 44100\,K + \lambda^2 + K\,\lambda^2}}$$

Using the fact that $1 \leq K < 1.000051$, we can then find that $|\tan(x_0)| > 210|\lambda|^{-1}$. Thus, for all values of $\lambda < 1$, we see that if $|\lambda \tan(x_0 + iy)| > 210$ and $|y| < .005$, then $|\lambda \tan(x_0)| > 210$ also.

Now we focus on the segment $[x_0 - r, x_0 + r]$ on the real axis. (Recall that $x_0 = \operatorname{Re} z_0$.) We will show that if $|T_\lambda(x_0)| > 205$, then the interval is mapped under T_λ to an interval of length greater than four. Such an interval must contain a pole, and thus the original pixel contained a part of $J(T_\lambda)$. (We note of course that we actually know that $|T_\lambda(x_0)| > 210$, but the weaker assumption that $|T_\lambda(x_0)| > 205$ will be used in the final case.)

We consider the width of the image of $[x_0 - r, x_0 + r]$ under T_λ, which is given by $|\lambda \tan(x_0 + r) - \lambda \tan(x_0 - r)|$, or the following:

$$\left|\lambda\left(\frac{\tan(r) - \tan(x_0)}{1 - \tan(r)\tan(x_0)} + \frac{\tan(r) - \tan(x_0)}{1 + \tan(r)\tan(x_0)}\right)\right| = \left|\lambda\frac{2\sin(2r)}{\cos(2r) + \cos(2x_0)}\right|$$

Then we note that, as $\cos(2r)$ is close to 1, while $\cos(2x_0)$ is close to -1, we must have

$$\left|\frac{2\lambda\sin(2r)}{\cos(2r) + \cos(2x_0)}\right| > \left|\frac{2\lambda\sin(2r)}{\cos(2x_0)}\right|$$

Finally, if we know that $|\lambda \tan(x_0)| > 205$, we know that $|\lambda/\cos(x_0)| > 205/|\sin(x_0)|$. Using this estimate allows us finally to get

$$|\lambda \tan(x_0 + r) - \lambda \tan(x_0 - r)| > \left|\frac{2\lambda \sin(2r)}{\cos(2x_0)}\right| \geq \left|\frac{410 \sin(2r)}{\sin(x_0)}\right| \geq 410 \sin(2r) > 4$$

Hence, the interval $[x_0 - r, x_0 + r]$ must be stretched to a length greater than π, and therefore it contains a pole of T_λ. This will suffice if the point z_0 escapes in a single iteration.

Lastly, we will consider the case where the pixel of radius r about z_0 intersects the real axis along $[x_0 - r, x_0 + r]$, and $|T_\lambda(z_0)| < 210$, but $|T_\lambda^n(z_0)| > 210$ for some $1 < n \leq N$. We will show that in fact such a pixel contains a point in the Julia set. We will do this in two stages. First, we will show that if we have $|T_\lambda^n(x_0)| > 205$, then either $[x_0 - r, x_0 + r]$ contains a point in $J(T_\lambda)$, or each of the intervals $[x_0 - r, x_0]$ and $[x_0, x_0 + r]$ expands under each iteration of T_λ. We assume that there is no point of $J(T_\lambda)$ contained in $[x_0 - r, x_0 + r]$, for if there is, we are done. We can now conclude that after $n - 1$ mappings, we had an interval of width at least $2r$ centered at $T_\lambda^{n-1}(x_0)$, so we have reverted to the case where z_0 escapes in a single iteration and we are done. Second, we will show that if $|T_\lambda^n(z_0)| > 210$, then for $m \leq n \leq N = 50$, we must have the real part of $T_\lambda^m(z_0)$ trapped in the interval $[T_\lambda^m(x_0 - r), T_\lambda^m(x_0 + r)]$. This will allow us to conclude that if $|T_\lambda^n(z_0)| > 210$, we must have either that $|T_\lambda^n(x_0)| > 205$, or that the interval $[T_\lambda^n(x_0 - r), T_\lambda^n(x_0 + r)]$ has length greater than five. If $|T_\lambda^n(x_0)| > 205$, then we will know that the interval $[x_0 - r, x_0 + r]$ has expanded, and we can revert to the case where z_0 escaped in a single iteration. In the second case, the interval $[x_0 - r, x_0 + r]$ has expanded to a length greater than five, and thus has encompassed a pole. In either case, we are done.

We will be able to assume throughout that the images $T_\lambda^n(z_0)$ have imaginary part between $\pm.005$. If we have an image $z_m = T_\lambda^m(z_0)$ with $|\operatorname{Im} z_m| \geq .005$, we would have the future images of z_0 trapped as before, and we could not have colored the pixel about z_0.

To carry out the proofs outlined above, we need to observe for $0 < \lambda < 1$ that $\lambda \tan(z) = z$ has two fixed points between $-\pi/2$ and $\pi/2$. Call these fixed points $\pm z_\lambda$. The segment $(-z_\lambda, z_\lambda)$ of the real axis between these two fixed points is in the attracting basin for the origin and maps into itself. (See figure 3.17.) Thus, if the entire interval $[x_0 - r, x_0 + r]$ is ever mapped into the segment $[-z_\lambda, z_\lambda]$ (or any π-translate), it will remain in this segment on future iterations.

The points $\pm z_\lambda$ are in fact repelling fixed points, and therefore in the Julia set $J(T_\lambda)$. We will show that z_λ is repelling, noting that a similar argument holds for $-z_\lambda$. Since $T_\lambda'(x) = \lambda \sec^2(x)$ is increasing for $0 < x < \pi/2$, we know that if $T'(z_\lambda) \leq 1$ then $T_\lambda'(x) < 1$ for $0 < x < z_\lambda$. But if $T_\lambda'(x) < 1$ on $[0, z_\lambda]$, then we have that $T_\lambda(z_\lambda) = \int_0^{z_\lambda} T_\lambda'(x)\, dx < \int_0^{z_\lambda} 1\, dx = z_\lambda$. However, $T_\lambda(z_\lambda) = z_\lambda$. Therefore, we see that we must have $T_\lambda'(z_\lambda) > 1$, and so z_λ is a repelling fixed point of T_λ.

Now we are ready to show that if $|T_\lambda^n(x_0)| > 205$, then either $[x_0 - r, x_0 + r]$ contains a point in $J(T_\lambda)$, or each of the intervals $[x_0 - r, x_0]$ and $[x_0, x_0 + r]$ expands under each iteration

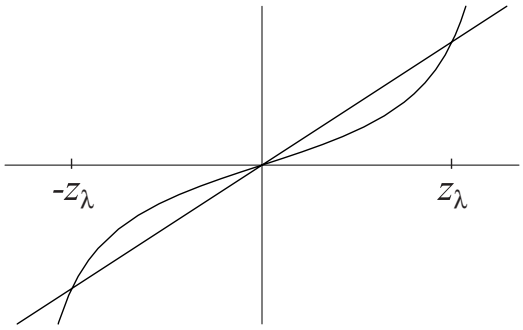

Figure 3.17: The fixed points $\pm z_\lambda$ for T_λ, and the attracting basin of the origin.

of T_λ. The segment $[x_0 - r, x_0 + r]$ may be in several locations in the interval $[-\pi/2, \pi/2]$, modulo π. First, it may be that the segment lies within the attracting basin $(-z_\lambda, z_\lambda)$. If it does, then all future iterates of x_0 will lie in this basin, contradicting our assumption that $|T_\lambda^n(x_0)| > 205$. It may alternatively be that a portion of the interval overlaps one of the points $\pm\pi/2$, but these points are in the Julia set as they are poles for T_λ, so that would mean that there was indeed a point of the Julia set in the interval. Similarly, if the interval overlaps one of the $\pm z_\lambda$, it also contains a point in the Julia set. Therefore we may assume that the interval lies entirely inside one of $(-\pi/2, -z_\lambda)$ or $(z_\lambda, \pi/2)$, modulo π. But we see by our analysis above of the fixed points z_λ that $|T'_\lambda(x)| > 1$ in these intervals, so the interval will expand when mapped by T_λ.

After the m^{th} iteration, if we do not have $|T_\lambda^m(x_0)| > 205$, the image of the interval has exactly the same options: either to overlap one of $\pm z_\lambda$ or $\pm\pi/2$ (modulo π) and therefore to contain a point of the Julia set; to become trapped in the attracting basin of the origin, and therefore never to have $|T_\lambda^n(x_0)| > 205$; or to expand on the next iteration. Thus we have shown that if $|T_\lambda^n(x_0)| > 205$, then either $[x_0 - r, x_0 + r]$ contains a point of $J(T_\lambda)$ or each of the intervals $[x_0 - r, x_0]$ and $[x_0, x_0 + r]$ expands under each iteration of T_λ.

To complete our proof for the case where z_0 takes more than one iteration to escape, all we need to do is to show that if we in fact have $|T_\lambda^n(z_0)| > 210$, we must have $|T_\lambda^n(x_0)| > 205$. To do this, we will show that $\operatorname{Re} T_\lambda^m(z_0)$ stays within the interval $[T_\lambda^m(x_0 - r), T_\lambda^m(x_0 + r)]$. We will not have to worry if the image of $[x_0 - r, x_0 + r]$ overlaps a pole of T_λ or a π-translate of the $\pm z_\lambda$; in this case the original pixel already contains a point in $J(T_\lambda)$ and we are done. Therefore we will assume that the images of the real interval $[x_0 - r, x_0 + r]$ never cross a pole or one of the repelling fixed points.

If it happens that the entire image of the real interval lands within the attracting basin $(-z_\lambda, z_\lambda)$, we know that the image of x_0 can never pass our bound. We need to consider however whether $T_\lambda^n(z_0)$ can still escape. Using an inductive argument, we assume that for $m < n$, we have thus far kept the real part of $T_\lambda^m(z_0)$ within $[T_\lambda^m(x_0 - r), T_\lambda^m(x_0 + r)]$, and we now have $\operatorname{Re} T_\lambda^{n-1}(z_0)$ within the attracting basin, modulo π. We observe that the vertical line with real part $x_{n-1} = \operatorname{Re} T_\lambda^{n-1}(z_0)$ will map under T_λ to a circle stretching between $\pm\lambda i$

and extending out to a real part no larger than $T_\lambda(x_{n-1})$ (see figure 3.6 in section 3.1). Since $|T_\lambda(x)| < |x|$ if $|x| < z_\lambda$, we see that the image $T_\lambda^n(z_0)$ will have real part between $\pm z_\lambda$ also. Thus, if the real interval $[x_0 - r, x_0 + r]$ gets mapped into the attracting basin, the image of z_0 also gets trapped, so we will not color the pixel.

So the only chance that the real part of the image of z_0 has of escaping from the image of the interval $[x_0 - r, x_0 + r]$ is to do so during a mapping from a π-translate of the intervals $(-\pi/2, -z_\lambda)$ or $(z_\lambda, \pi/2)$. We consider the mapping of $T_\lambda^{m-1}(x_0 - r)$, $T_\lambda^{m-1}(z_0)$, and $T_\lambda^{m-1}(x_0 + r)$ in the next iteration, using our assumption that there are no poles or repelling fixed points between the images. We can assume without loss of generality that we are working with real part between $\pm\pi/2$. We then note by the mapping properties already discussed for vertical lines that in the next iteration the distance between the real part of the image of z_0 and the endpoint farther from the origin will increase. (Consider for example, three points $0 < a < b < c < \pi/2$; then $\mathrm{Re}\, T_\lambda(b + iy) < T_\lambda(b) < T_\lambda(c)$; see figure 3.18.) So

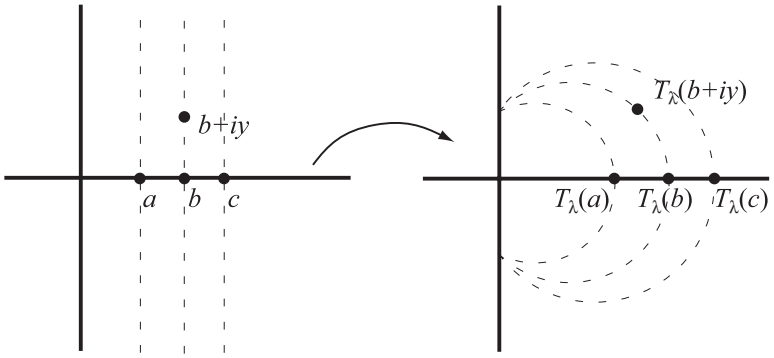

Figure 3.18: With three points $0 < a < b < c < \pi/2$, we have $\mathrm{Re}\, T_\lambda(b + iy) < T_\lambda(b) < T_\lambda(c)$. (The real part of the image of $b + iy$ moves back from the image of b if we include any imaginary part.)

this endpoint does not occasion concern. However, it does appear that the distance between the real part of the image of z_0 and the smaller of the two endpoints could decrease. In fact it seems conceivable that we could end up with the real part of the next image of z_0 actually closer to the origin than the image of this smaller endpoint; in this case, $\mathrm{Re}\, T_\lambda^n(z_0) \notin [T_\lambda^n(x_0 - r), T_\lambda^n(x_0 + r)]$, which we wish to prevent. (Considering our three points a, b, and c again, it is clear that $T_\lambda(a) < T_\lambda(b)$, but it is also clear that $\mathrm{Re}\, T_\lambda(b + iy) < T_\lambda(b)$, and it may be that $\mathrm{Re}\, T_\lambda(b + iy) < T_\lambda(a)$. See figure 3.19.)

We are however protected by the fact that all images of z_0 must have an imaginary part less than .005. This will restrict how far back $\mathrm{Re}\, T_\lambda(x + iy)$ may be from $T_\lambda(x)$. We note that the difference $|T_\lambda(x) - T_\lambda(x + iy)|$ is greatest when the image $T_\lambda(x + iy)$ has imaginary part as large as possible. In our situation, this means that the imaginary part of the image is .005. It is also clear that for the largest change in real part, we want the vertical line through our point to map to a circle with the largest possible curvature; that is, the circle with the smallest radius. At first, this appears to be a problem, since the smallest radius

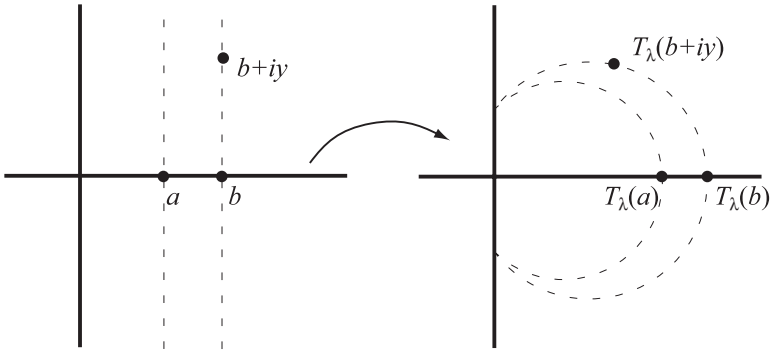

Figure 3.19: For $0 < a < b < \pi/2$, it could be that $\operatorname{Re} T_\lambda(b+iy) < T_\lambda(a)$.

circle resulting from a vertical line under the map T_λ has a radius of λ. (The smallest radius circle corresponds to a half-circle passing through $\pm\lambda i$ and λ. See figure 3.20.) Since λ can have any value greater than 0, we can have arbitrarily large curvature, which could make it difficult to determine how far back $T_\lambda(x+iy)$ may have moved from $T_\lambda(x)$.

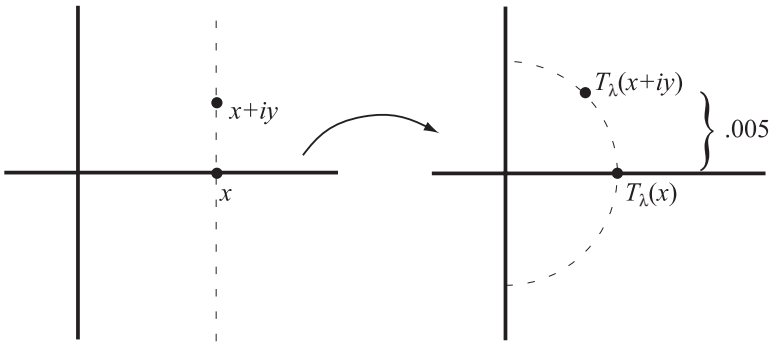

Figure 3.20: For a fixed λ, the greatest backward movement in the real part of $T_\lambda(x+iy)$ results from the half-circle of radius λ. We need only compute how far back we may take the real part by adding an imaginary part of .005.

It turns out that we do not have to worry about small λ. When λ is small, the fixed point z_λ is large. As a result, for small values of λ, the image of $\operatorname{Re} z = x$ under T_λ will have maximum curvature only when we have an x which is inside the attracting basin for the origin. We have already dealt with this case and shown that the image of z_0 will then never map past our real bound. Therefore, we need only deal with values of λ larger than that required for the fixed point z_λ to be at least as large as λ.

When $\lambda = .7$, we can compute that $z_{(.7)} > .92$. (We can tell this because $.7\tan(.92) \approx .919284 < .92$.) Therefore, the curvature corresponding to a circle of radius .7 is greater than the largest curvature we will have to consider. In the case where $\lambda = .7$, the image of z_0 moves up along a circle of radius .7 about the origin, so we see that we can move at most a distance $.7 - \sqrt{.7^2 - .005^2} < .00002$ closer to the origin. (See figure 3.20.) We know from

our previous argument that the interval we are working on is expanding, so our endpoints have not gotten closer to the image of the real part in the previous iteration. Therefore, the real part of the image of z_0 can move no more than .00002 closer to either endpoint of the image of $[x_0 - r, x_0 + r]$ at each stage. After fifty iterations, we must therefore still have $T_\lambda^{50}(z_0)$ a distance of at least .001 from the endpoints of the image of $[x_0 - r, x_0 + r]$.

So we are back to our first case, because we have now an interval $[T_\lambda^n(x_0) - r, T_\lambda^n(x_0) + r]$ which is in the image of the original pixel. Since $|T_\lambda^n(z_0)| > 210$, and $\operatorname{Re} T_\lambda^n(z_0) \in [T_\lambda^n(x_0 - r), T_\lambda^n(x_0 + r)]$, we know that either $|T_\lambda^n(x_0)| > 205$, in which case we know that the interval $[T_\lambda^n(x_0) - r, T_\lambda^n(x_0) + r]$ will expand to include a pole, or the interval $[T_\lambda^n(x_0 - r), T_\lambda^n(x_0 + r)]$ has length greater than five, and hence contains a pole. Either way, there is a part of $J(T_\lambda)$ in the original pixel.

Thus we have completed the proof, and we see that $J_c(T_\lambda)$ is accurate. ■

Chapter 4

An Inaccurate Representation of a Julia Set

We consider the family given by

$$G_\lambda(z) = \frac{\lambda e^z}{e^z - e^{-z}}$$

for $\lambda > 0$. The algorithm we used for the family $\lambda \tan(z)$ will produce incorrect results for this family with some reasonable choices of parameters. We note that the Schwarzian derivative of G_λ is -2, so Theorem 2 does apply.

4.1 Mapping Properties

As in the case for tangent, we rewrite the function as a composition of an exponential map with a Möbius transformation to discuss the mapping properties. In this case, we have $G_\lambda(z) = \lambda L(e^{-2z})$ where

$$L(z) = \frac{1}{1-z}$$

We can now determine the mapping properties of $G_\lambda(z)$, as we did with T_λ.

We start with a point $z = x + iy$ in the complex plane. We see that $e^{-2z} = e^{-2(x+iy)} = e^{-2x}\left[\cos(-2y) + i\sin(-2y)\right]$. Letting $r = e^{-2x}$ and $\theta = -2y$, we plug into $\lambda L(z)$ and simplify, finding the real and imaginary parts of the image as follows:

$$\frac{\lambda}{1 - r\cos(\theta) - ir\sin(\theta)} = \lambda\frac{1 - r\cos(\theta)}{1 + r^2 - 2r\cos(\theta)} + i\,\lambda\frac{r\sin(\theta)}{1 + r^2 - 2r\cos(\theta)} \tag{4.1}$$

Next consider a horizontal line $x + iy_0$ with imaginary part y_0. These are mapped by e^{-2z} to rays extending from the origin which make an angle $-2y_0$ with the real axis. Then we

consider the action of the Möbius transformation $\lambda L(z)$ on the three points 0, ∞, and $e^{i\theta}$, where $\theta = -2y$. We have $\lambda L(0) = \lambda$ and $\lambda L(\infty) = 0$. Using the real and imaginary parts from equation (4.1) above with $r = 1$, we see that

$$\lambda L(e^{i\theta}) = \lambda \frac{1 - \cos(\theta)}{2 - 2\cos(\theta)} + \lambda\, i \frac{\sin(\theta)}{2 - 2\cos(\theta)}$$

We see then that the real part is always $\lambda/2$, and that the imaginary part is nonzero so long as $\sin(\theta) \neq 0$. Thus, we have the horizontal line $x + iy_0$ mapping to a circular arc connecting λ and 0, so long as θ is not a multiple of π. If θ is a multiple of π, then the imaginary part is zero and we have only a line segment. The arc lies above or below the axis according the whether $\sin(-2y)$ is positive or negative.

We can now see the two asymptotic values for G_λ. If we allow $\operatorname{Re} z$ to go towards infinity in the positive direction, then we see the real part in (4.1) goes to λ while the imaginary part goes to zero. If instead we allow $\operatorname{Re} z$ to go towards infinity in the negative direction, then the real and imaginary parts of $G_\lambda(z)$ both go to zero. Thus, 0 and λ are both asymptotic values for $G_\lambda(z)$. Since the family $G_\lambda(z)$ has a constant Schwarzian derivative, there are exactly 2 asymptotic values, so we have found them all.

4.2 The Fatou and Julia Sets

We are now able to sketch out a few properties of the Fatou and Julia sets for the family G_λ. We will however not develop very precise descriptions of either.

If we start with a vertical line $x_0 + iy$ with $x_0 > 0$, then this maps under e^{-2z} to circle with radius $r < 1$. This means that when we plug into the real part of equation (4.1) above, we get numbers which are strictly positive. Therefore we see that the right half plane maps into the right half plane. We therefore have a family of meromorphic functions which miss more than three points, and so by Montel the right half plane is in the Fatou set for G_λ. In fact, Devaney and Keen [11] noted that there is a real attracting fixed point q in the right half plane, and by applying the Schwarz Lemma, we can see that $G_\lambda^n(z) \to q$ as $n \to \infty$. Devaney and Keen also showed that the negative real axis is in the Julia set. The origin can be easily shown to be in the Julia set as 0 is a pole of $G_\lambda(z)$. (We noted above that 0 was also an asymptotic value. Some of the unusual behavior of this function is a result of this fact, as we will discuss later.)

So we know by invariance that if a point passes into the right half plane, this point is in the Fatou set. We will therefore consider what points from the left half plane map into the right-half plane in the first iteration. If we again let $r = e^{-2x}$ and $\theta = -2y$, then we have

$$\operatorname{Re}\, G_\lambda(x + iy) = \lambda \frac{1 - r\cos(\theta)}{1 - 2r\cos(\theta) + r^2}$$

and this crosses the imaginary axis into the left half plane only when $\theta = 2n\pi$ or $y = n\pi$ (which corresponds to the origin), and also when $r = \sec(\theta)$. We think again of horizontal lines mapping to arcs between 0 and λ. If the arc has radius smaller than $\lambda/2$, then the arc lies entirely in the right half plane. If the radius is greater than $\lambda/2$, then the leftmost section of the arc lies in the left half plane. Noting that $\theta = -2y$, we have curves $e^{-2x} = \sec(\theta)$ which bound the Julia set in the left half plane, since past this point, horizontal lines are being mapped to arcs in the right half plane. Because $e^{-2x} \geq 0$, we know that these curves are restricted to the region where $-\pi/4 \leq y \leq \pi/4$ (modulo π). In particular, the region from $\pi/4 \leq y \leq 3\pi/4$ must be contained in the Fatou set. Figure 4.1 illustrates the situation. We

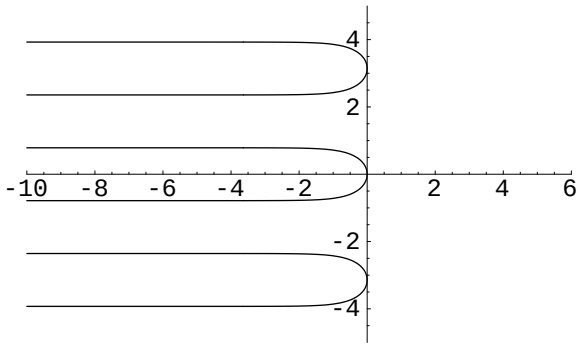

Figure 4.1: The Julia set for G_1 must be contained inside curves in the left half plane such as the ones shown here.

note that our regions do include the negative real axis.

4.3 An Inaccurate Representation

Finally we wish to consider the accuracy of computed Julia sets for this function. Since it is meromorphic function with polynomial Schwarzian derivative, we could use Theorem 2 as we have before to design our algorithm. Again we would select a window, a pixel width, a maximum number of iterations N, and a bound B, iterating the point z_0 in the center of a pixel and coloring the pixel only if $|G_\lambda^n(z_0)| > B$ for $n \leq N$. Since we already know that the right half plane is entirely contained in the Fatou set, it makes sense to only look at a window W which covers a region in the left half plane. In the imaginary direction, we might include a region such $\{z : |\mathrm{Im}\, z| < \pi\}$ since the function is clearly $2\pi i$ periodic. Let us suppose then we wish to look at a window that covers the region $\{x + iy : -10 \leq x \leq 0, |y| < \pi\}$.

If we consider the line $\mathrm{Im}\, z = \pi/2$, we know from the previous section that this must be contained within the Fatou set, and that the closest any part of the Julia set may be to the line is $\pi/4$. Thus any pixels centered on this line with radius less than $\pi/4 \approx 0.7854$ will be entirely in $F(G_\lambda)$. However, we may compute approximate values to the first and second iterates for some points along the line $\mathrm{Im}\, z = \pi/2$ as follows:

z	$G_\lambda(z)$	$G_\lambda^2(z)$
$-3. + 1.5708i$	$.002473 + 1.812 \times 10^{-8}i$	$202.7 - .001482i$
$-5 + 1.5708i$	$.00004540 + 3.335 \times 10^{-10}i$	$1.101 \times 10^5 - .08091i$
$-7 + 1.5708i$	$8.315 \times 10^{-7} + 6.109 \times 10^{-12}i$	$6.013 \times 10^6 - 4.417i$
$-10 + 1.5708i$	$2.061 \times 10^{-9} + 1.514 \times 10^{-14}i$	$2.426 \times 10^8 - 1.782 \times 10^4 i$

It becomes apparent that the modulus of the second iterate is growing large very quickly as we move in the negative direction. If we have pixels centered at z with real parts less than -3, we would need a bound of greater than 203 to avoid coloring pixels with imaginary part 1.5708; by the time the real part is as small as -10, we need a bound larger than 10^8, which is quite large. These values are likely larger than we would intuitively select for B.

What is happening here is seen from the first column of the table. It is the fact that 0 is both an asymptotic value and a pole that is causing the problem. As the real part of our point moves towards negative infinity, we see that $G_\lambda(z)$ moves closer to zero. But zero is a pole, so the closer $G_\lambda(z)$ is to zero, the larger the image $G_\lambda^2(z)$ must become.

We note however, that all of our computed second iterates remain in the right half plane, as we know they must. On subsequent iterations, they will in fact approach the attracting fixed point on the real axis. Thus, no point in the left half plane actually tends to infinity under iteration, but our algorithm can produce inaccurate results because for any given B, there exists some point z_B in the Fatou set for which $|G_\lambda^2(z_B)| > B$.

Chapter 5

Conclusions

In considering computed Julia sets, we have found in some cases that "reasonable" choices of parameters for our algorithms result in accurate representations, while in other cases we may get inaccurate representations. In both cases we are left with the difficulty of determining what constitutes "reasonable" choices for our parameters. We also face the difficulty of coming up with an algorithm which could be used to produce pictures of the Julia set. The back iteration process discussed in section 1.1 is the most general algorithm, but has drawbacks in implementation. Reasonably simple algorithms exist for some functions, such as the algorithm used in Chapter 2 to find points in $J(E_\lambda)$ by looking for those points which move toward infinity in the real direction. The algorithm based on Theorem 2 which we used for functions with polynomial Schwarzian derivatives is similar, allowing us to look for points which move toward infinity. Both are reminiscent of the most common algorithm for polynomials, in which we find the Julia set by looking at the boundary of those points which go to infinity under iteration.

5.1 Problems with the Algorithms

We are faced with two different problems in our algorithms. First, we are representing an entire rectangle or pixel with a single point. We color the rectangle based on the behavior of this single point. In some sense, we are assuming that the behavior of a set of points close to each other will be roughly the same under iteration. Of course, the assumption is essentially that the iterates of the function form a normal family in this region, which is exactly what is *not* true if we are working in the Julia set.

Second, we are trying to predict the long term behavior of a point based on a finite number of iterations. Usually this takes the form of trying to determine whether or not a point will go to infinity under iteration by looking at the first N iterates and deciding whether or not they are "large" in some sense. So we find ourselves in the uncomfortable position of guessing the

limit of a sequence from looking at the first N terms. In the popular case of the iteration of quadratic polynomials $z^2 + c$, the trick used to overcome this problem is to note that if $|z| > 2$, then the iterates $z_n \to \infty$. This results in a simple criterion to determine whether or not a point will go to infinity: color a pixel centered at z_0 if the first N iterates of z_0 have modulus less than 2. The result also implies that these Julia sets are bounded. In the general case of functions meromorphic in the complex plane, we have no similar guarantees. In general, both the Fatou and Julia sets of such functions may be unbounded.

To some degree, the second problem actually offsets the first. If we are only working with the first N iterates of a function, we then have a *finite* family of iterates. A finite family of functions continuous at a point z_0 will indeed be equicontinuous at that point. (For any $\epsilon > 0$, there exists a δ_n such that if $|z - z_0| < \delta_n$, $|f^n(z) - f^n(z_0)| < \epsilon$. Then to have equicontinuity for the family $\{f^n\}$, $n \leq N$ at z_0, simply let $\delta = \min\{\delta_n\}$.) Equicontinuity is only lost when we are dealing with infinitely many iterates. Thus we have somewhat similar behavior in the first N iterations over a sufficiently small region, even if that region includes parts of $J(f)$.

The analysis we have carried out in determining whether or not $J_c(f)$ is accurate or not is an attempt to deal with the first problem. In essence we have said that we have an accurate representation if the determining point z_0 at the center of the pixel behaves like a point in the Julia set (by becoming large on iteration) only if there is a point in the Julia set nearby.

The problems also affect our choice of parameters. In dealing with the family $E_\lambda(z) = \lambda e^z$, we found that the choice of both the window W and the bound B affects the picture we get. In this family, points with real part less than 1 never get mapped past our bound, which means that the entire region to left of the line $\operatorname{Re} z = 1$ remains uncolored. It also means that these points are in fact in the Fatou set. In this case, the behavior of the finite family is essentially the same as the infinite family. Similarly, a small λ could require a larger W to see any parts of the Julia set. However, we may be concerned if our window W is quite large, that a small bound may map regions in the Fatou set past our bound.

A similar situation results in the case of $T_\lambda(z)$. As a trivial example, if our algorithm checks the modulus of $z_i = f^i(z_0)$ before iterating, we would need to choose W so that we have $|z_0| < B$ for the center z_0 of any pixel. This affects our choice of W. (We will likely avoid this by iterating once first, and only check the modulus of z_i for $i \geq 1$.) More realistically, we also discussed in section 3.4 that if we work with large λ, we must increase our bound B if the computed Julia set is to remain accurate. As we discussed, there is some intuitive notion that since we are judging whether a point goes to infinity by how large it becomes, we must consider what we should call "large" for a given function.

We have mostly ignored the fact that pixels containing the Julia set may *not* be colored; this criterion was not part of our definition of accuracy. Attempting to include such a criterion is doomed, since the Julia set in general will include repelling fixed points, and if we happen to iterate such a point, it will definitely not tend to infinity. (The repelling periodic points are in fact dense in the Julia sets for all the functions we have considered.) Thus for example,

if we divide up the window to create a computed Julia set for T_λ in such a way that that one pixel has center at $z_0 = 0$, we see that this pixel will *not* be colored: $T_\lambda(0) = 0$. So our computed Julia set would then show a gap in the real axis near the origin. In fact, it will be possible for other points close to the origin not to be mapped past our real bound within fifty iterations. Consider for example that we showed $T_1^{50}(.01) < .07$. (See Appendix A.) Thus again we would clearly have a gap about the origin in our computed Julia set. This gap is misleading since in fact $J(T_1)$ is the entire real axis.

5.2 Problems with Functions

We also have the explicit problem of inaccurate Julia sets such as the one we discussed in Chapter 4. Here, the problem results from the fact that one asymptotic value is also a pole. Generally we may in expect problems with the accuracy of computed Julia sets for transcendental meromorphic functions some of whose asymptotic values are poles, but for which the Julia set is not the entire plane. At least we would expect problems when there is a reasonably wide strip in which $f(z)$ approaches the asymptotic value as z goes to infinity. In this case, we will have a strip with infinity as a boundary point mapped very close to the asymptotic value in the first iteration. Since this asymptotic value is also a pole, this large open set is mapped to a region with large modulus in the second iteration. The further out we go in the asymptotic tract, the closer to the pole the image of the region will be, and the larger the second iteration will consequently be. We may also expect that at least some pixels in this set will be entirely in the Fatou set, as was true in our example.

In some sense, this is extremely bad behavior; points are first mapped very close together and then mapped close to the essential singularity at infinity. In our case, had both asymptotic values been poles, we would have had that the entire plane is the Julia set [11]. So in some sense, we might describe the case where one asymptotic value is a pole and the other is not as being "halfway" to having a Julia set which is the entire plane. In other words, even the Fatou set is "badly" behaved.

5.3 Suggestions

In general, we find that a straightforward algorithm may not be appropriate for a large classes of functions. We may need more specific details about the functions. Using an algorithm such as ours and choosing a "large" value for a bound B, and an appropriate choice for W and even N may depend on the specifics of the function involved. Simply picking "obvious" candidates for these values may not work.

In addition, we would need to develop algorithms for general functions. We have developed an algorithm for functions with polynomial Schwarzian derivatives, but this was dependent on

several very special features of these functions, such as the fact that they have neither Baker domains nor wandering domains. (Of course, we also subsequently demonstrated that this algorithm may not produce accurate pictures.) For a general transcendental meromorphic function, we do have Domínguez' result [12] that the Julia set is the boundary of points which go to infinity. Such a criteria has been used commonly with polynomials, producing pictures of a so-called "filled in" Julia set. We could reasonably do the same for meromorphic functions.

Alternately, we could use the method of back iteration. There is an inherent sense of stability in such algorithms from the fact that *any* non-exceptional point will tend towards the Julia set under back iteration, so we may expect small errors to be wiped out. Such algorithms are harder to implement than the algorithms discussed in this paper. For such algorithms, we must calculate an inverse (which may be difficult), we must keep track of a large number of points, and we have no guarantees about which parts of the Julia set will be revealed. Although the backwards orbit will at some point come close to every point in the Julia set, we have no idea how long it may take, and some regions get visited more often than others. The last problem is related to one of the problems we have already run into; we are trying to substitute a finite process for an infinite one.

There is hope for our algorithms. We have shown them to produce accurate pictures in some cases. We could conceivably reproduce such an argument for whatever function we are interested in. However, developing an explicit argument may be considerably harder for other families of functions, so showing accuracy for a given family before generating pictures may not be feasible. We may do best by being on the lookout for special cases, such as when an asymptotic value is also a pole, and be aware that for such cases it will be particularly hard to develop accurate pictures.

Bibliography

[1] I. N. Baker. Repulsive fixpoints of entire functions. *Mathematische Zeitschrift*, 104:252–256, 1968.

[2] I. N. Baker. An entire function which has wandering domains. *Journal of the Australian Mathematical Society Series A*, 22:173–176, 1976.

[3] I. N. Baker and P. Domínguez. Boundaries of unbounded Fatou components of entire functions. *Annales Academiæ Scientiarum Fennicæ*, 24:437–464, 1999.

[4] I. N. Baker, J. Kotus, and Lü Yinian. Iterates of meromorphic functions II: Examples of wandering domains. *Journal of the London Mathematical Society*, 2(42):267–278, 1990.

[5] I. N. Baker, J. Kotus, and Lü Yinian. Iterates of meromorphic functions: I. *Ergodic Theory and Dynamical Systems*, 11:241–248, 1991.

[6] I. N. Baker, J. Kotus, and Lü Yinian. Iterates of meromorphic functions III: Preperiodic domains. *Ergodic Theory and Dynamical Systems*, 11:603–618, 1991.

[7] Alan F. Beardon. *Iteration of Rational Functions: Complex Analytic Dynamical Systems*. Number 132 in Graduate Texts in Mathematics. Springer-Verlag, New York, 1991.

[8] Walter Bergweiler. Iteration of meromorphic functions. *Bulletin of the American Mathematical Society*, 29:151–188, 1993.

[9] Paul Blanchard. Complex analytic dynamics on the Riemann sphere. *Bulletin (new Series) of the American Mathematical Society*, 11(1):85–140, July 1984.

[10] Robert L. Devaney and Marilyn B. Durkin. The exploding exponential and other chaotic bursts in complex dynamics. *American Mathematical Monthly*, 98:217–233, 1991.

[11] Robert L. Devaney and Linda Keen. Dynamics of meromorphic maps: Maps with polynomial Schwarzian derivative. *Annales Scientifiques de L'École Normale Supérieure*, 4(22):55–79, 1989.

[12] P. Domínguez. Dynamics of transcendental meromorphic functions. *Annales Academiæ-Scientiarum Fennicæ*, 23:225–250, 1998.

[13] Marilyn B. Durkin. The accuracy of computer algorithms in dynamical systems. *International Journal of Bifurcation and Chaos*, 1(3):625–639, 1991.

[14] A. E. Eremenko. On the iteration of entire functions. In *Dynamical Systems and Ergodic Theory*, volume 23 of *Banach Series Publications*, pages 339–345, Warszawa, 1989. Polish Scientific Publishers.

[15] A. E. Eremenko and M. Ju. Ljubich. Examples of entire functions with pathological dynamics. *Journal of the London Mathematical Society*, 2(36):458–468, 1987.

[16] Paul Fatou. Sur les équations fonctionelles. *Bulletin de la Société Mathématíque de France*, 48, 49:161–271, 33–94, 208–314, 1919, 1920.

[17] Zhang Guan-Hou. *Theory of Entire and meromorphic functions: Deficient and Asymptotic Values and Singular Directions*, volume 122 of *Translations of Mathematical Monographs*. American Mathematical Society, Providence, Rhode Island, 1993.

[18] W. K. Hayman. *Meromorphic Functions*. Oxford mathematical monographs. Oxford, Clarendon Press, 1964.

[19] L. Keen and J. Kotus. Dynamics of the family $\lambda \tan(z)$. *Conformal Geometry and Dynamics*, 1:28–57, August 1997. An electronic journal of the American Mathematical Society.

[20] H. O. Peitgen. *The Science of fractal images*, chapter 4. Springer-Verlag, 1988.

[21] Dietmar Saupé. Efficient computation of Julia sets and their fractal dimension. *Physica*, 28D:358–70, 1987.

[22] Joel L. Schiff. *Normal Families*. Springer-Verlag, New York, 1993.

[23] Norbert Steinmetz. *Rational Iteration: Complex Analytic Dynamical Systems*. Number 16 in de Gruyter Studies in Mathematics. Walter de Gruyter & Co., Berlin, 1993.

[24] Dennis Sullivan. Quasiconformal homeomorphisms and dynamics I. solution of the Fatou-Julia problem on wandering domains. *Annals of Mathematics*, 122(2):401–418, 1985.

Appendix A

Some Numerical Calculations

The work in this document requires a large number of approximations. Some were straightforward, and details were sometimes included. In other cases, standard software could be used to approximate more complicated quantities. Two approximations in particular caused problems, however, because they required approximating the value of iteration. Small errors are not a problem when we do a single calculation, as long as we do not require a large number of correct digits. However, in an iterative process, small errors may propagate and cause serious problems in the output.

The approach we take to make these estimates is as follows. We will make an approximation to the first iterate using built-in functions from the software Matlab. We then add a certain amount of error in the appropriate direction before computing the second iterate. The error is added to be sure that any errors in our computations result in a quantity bigger (or smaller) than the actual quantity, so that our final answer will be guaranteed to be a lower (upper) bound on the actual value.

We begin with the following estimate, required in 3.5: We will show that the forty-ninth iterate of $\tan(z)$ applied to the point $x = .01$ does not move past 1.56. We do this by calculating $\tan(z)$ at each stage, and assuming that the answer we get is correct to at least four digits (for the input we used). We then note that as $\tan(z)$ is increasing, adding some amount to the result will only increase our final answer. Therefore, we add .001 to the result before calculating the correct iterate. We get a series of approximations $x'_0, x'_1, \ldots, x'_{49}$ to the actual iterates $x_0, x_1, \ldots, x_{49}$ with the property that $x_0 = x'_0 = .01$ and $x_n < x'_n$ for $n > 0$. The code used in Matlab follows:

```
x(1) = .01;
for i=1:49
     x(i+1) = tan(x(i)) + .001;
end
x'
```

The output is as follows:

```
0.0100
0.0110
0.0120
0.0130
0.0140
0.0150
0.0160
0.0170
0.0180
0.0190
0.0200
0.0210
0.0220
0.0230
0.0240
0.0250
0.0260
0.0270
0.0280
0.0291
0.0301
0.0311
0.0321
0.0331
0.0341
0.0351
0.0361
0.0371
0.0382
0.0392
0.0402
0.0412
0.0422
0.0433
0.0443
0.0453
0.0464
0.0474
0.0484
0.0495
```

```
0.0505
0.0516
0.0526
0.0536
0.0547
0.0558
0.0568
0.0579
0.0589
0.0600
```

Similarly, we need to show that arctan iterated fifty times at the point 1.566 is no smaller than .17. (This is needed in section 3.3.) We work as before, this time subtracting .0001 from each approximation, and noting that this will only make our final answer smaller. The code is as follows:

```
x(1) = 1.566;
for i=1:49
     x(i+1) = atan(x(i))-.0001;
end
x'
```

The output follows:

```
1.5660
1.0024
0.7865
0.6664
0.5877
0.5312
0.4882
0.4541
0.4261
0.4027
0.3828
0.3655
0.3503
0.3368
0.3248
0.3139
0.3041
```

```
0.2951
0.2869
0.2793
0.2722
0.2657
0.2596
0.2539
0.2485
0.2435
0.2387
0.2343
0.2300
0.2260
0.2221
0.2185
0.2150
0.2117
0.2085
0.2055
0.2025
0.1997
0.1970
0.1945
0.1920
0.1895
0.1872
0.1850
0.1828
0.1807
0.1787
0.1767
0.1748
0.1730
```

It is therefore clear that the result is in fact larger than .17, and the result is achieved.

We need a somewhat stronger result in section 3.4, namely that $T_\lambda^{-50}(1.566)$ is greater than .17 so long as $\lambda < 1.00001$, but the modifications are simple to make:

```
x(1) = 1.566;
for i=1:49
     x(i+1) = atan(x(i))/1.00001-.0001;
```

```
end
x'
```

The results are similar to those before:

```
1.5660
1.0024
0.7865
0.6663
0.5877
0.5312
0.4882
0.4540
0.4261
0.4027
0.3827
0.3654
0.3503
0.3368
0.3248
0.3139
0.3041
0.2951
0.2868
0.2792
0.2722
0.2657
0.2596
0.2538
0.2485
0.2435
0.2387
0.2342
0.2300
0.2259
0.2221
0.2185
0.2150
0.2117
0.2085
0.2054
0.2025
```

```
0.1997
0.1970
0.1944
0.1919
0.1895
0.1872
0.1849
0.1828
0.1807
0.1786
0.1767
0.1748
0.1729
```

Vita

John Hoggard was born in 1971 in Indiana, but grew up mostly in Texas. He went to Oberlin College, graduating with honors in 1993. He then went to Blacksburg to attend Virginia Tech, earning a Masters in Mathematics in 1995, and a Ph.D. in the summer of 2000.